Copyright Warning & Restrictions

The copyright law of the United States (Title 17, United States Code) governs the making of photocopies or other reproductions of copyrighted material.

Under certain conditions specified in the law, libraries and archives are authorized to furnish a photocopy or other reproduction. One of these specified conditions is that the photocopy or reproduction is not to be "used for any purpose other than private study, scholarship, or research." If a, user makes a request for, or later uses, a photocopy or reproduction for purposes in excess of "fair use" that user may be liable for copyright infringement,

This institution reserves the right to refuse to accept a copying order if, in its judgment, fulfillment of the order would involve violation of copyright law.

Please Note: The author retains the copyright while the New Jersey Institute of Technology reserves the right to distribute this thesis or dissertation

Printing note: If you do not wish to print this page, then select "Pages from: first page # to: last page #" on the print dialog screen

ABSTRACT

STABILITY AND PRECIPITATION OF DIVERSE NANOPARTICLES

by
Chintal Desai

Nanotechnology is a rapidly growing industry that is exploiting the novel characteristics of materials manufactured at the nanoscale. Carbon based nanomaterials such as Carbon Nanotubes (CNTs) and Detonation Nanodiamond (DND) possess unique properties and find a wide range of industrial applications. With the advent of mass production of such materials, there is a possibility of contamination of water resources. Depending on the surface properties and structures, they might aggregate and settle down, or be dispersed and transported by the water. Therefore, there is a need to develop an understanding of the fate of such materials in aqueous media. The understanding and effect of solution chemistry is a key to predicting their deposition, transport, reactivity, and bioavailability in aquatic environments.

The colloidal behavior of organic dispersed CNTs and water dispersed DNDs is investigated. The aggregation behavior of these two colloidal systems is quite different from that of hydrophilic, water soluble functionalized CNTs (F-CNTs). The values of the Fuchs stability ratio or the critical coagulant concentration are determined experimentally using time-resolved dynamic light scattering and are used to predict the stability of such systems. It is found that the aggregation behavior of the organic dispersed, antisolvent precipitated system does not follow the conventional Derjaguin–Landau–Verwey–Overbeek (DLVO) theory. But they stabilize in the long term, which is attributed to the supersaturation generated by different solubility of a solute in the solvent/antisolvent.

Based on particle size distribution, zeta potential as well as the aggregation kinetics, the water dispersed DNDs are found to be relatively stable in aqueous solutions, but aggregate rapidly in presence of mono and divalent salts. Also, the formation of carboxylic groups on the DND surface does not alter colloidal behavior as dramatically as it does for other nanocarbons especially carbon nanotubes.

Formation of colloidal dispersions via precipitation processes has been widely used in the chemical and pharmaceutical industries. The synthesis of micro- particles for hydrophobic drugs is effectively carried out via anti-solvent precipitation method. The formation of small particles in the precipitation method is strongly influenced by colloidal interactions, and therefore, dependent on the properties of the particles and the liquid. The effect of solvent on the colloidal stability of the micro-drug particles is studied in detail. It is found that the organic solvent plays an important role on particle formation, polymorphism and stability of micron scale drug particles in aqueous media. Also, the supersaturation can be varied by using different solvents and the physicochemical characteristics of the suspension can be altered, which affects stability. Understanding of the colloidal stability and the aggregation kinetics has great importance not only for fundamental researches, but also for their applications.

STABILITY AND PRECIPITATION OF DIVERSE NANOPARTICLES

by
Chintal Desai

A Dissertation
Submitted to the Faculty of
New Jersey Institute of Technology
in Partial Fulfillment of the Requirements for the Degree of
Doctor of Philosophy in Chemistry

Department of Chemistry and Environmental Science

May 2013

.

APPROVAL PAGE

STABILITY AND PRECIPITATION OF DIVERSE NANOPARTICLES

Chintal Desai

Dr. Somenath Mitra, Dissertation Advisor — Date
Distinguished Professor of Chemistry and Environmental Science, NJIT

Dr. Carol A. Venanzi, Committee Member — Date
Distinguished Professor of Chemistry and Environmental Science, NJIT

Dr. Edgardo Farinas, Committee Member — Date
Associate Professor of Chemistry and Environmental Science, NJIT

Dr. Haidong Huang, Committee Member — Date
Assistant Professor of Chemistry and Environmental Science, NJIT

Dr. Pradyot Patnaik, Committee Member — Date
Consultant, Radiance, Burlington, New Jersey

BIOGRAPHICAL SKETCH

Author: Chintal Desai

Degree: Doctor of Philosophy

Date: May 2013

Undergraduate and Graduate Education:

- Doctor of Philosophy in Chemistry,
  New Jersey Institute of Technology, Newark, NJ, 2013

- Master of Science in Chemistry,
  South Gujarat University, Surat, India, 1997

- Bachelor of Science in Chemistry,
  B. P. Baria Science Institute, Navsari, India, 1995

Major: Chemistry

Peer Reviewed Publications:

Desai, C., Mitra, S. 2013. Aggregation behavior of detonation nanodiamonds and their functionalized analog in aqueous environment. (In preparation)

Desai, C., Mitra, S. 2013. Microwave induced carboxylation of nanodiamonds. Diamond and Related Materials. 34, 65-69.

Lau, X., Desai, C., Mitra, S. 2013. Functionalized nanodiamond as a charge transporter in organic solar cells. Solar Energy. 91, 204-211.

Roy, S., Mitra, K., Desai, C., Mitra. S. 2013. Detonation nanodiamonds and carbon nanotubes as reinforcements in epoxy composites- A Comparative study. Journal of Nanotechnology in Engineering and Medicine. (Under Review).

Addo Ntim, S., Sae-Khow, O., Desai, C., Mitra, S. 2012 Size dependent aqueous dispersibility of carboxylated multiwall carbon nanotubes. Journal of Environmental Monitoring. 14, 2772-2779.

Desai, C., Addo Ntim, S., Mitra, S. Antisolvent precipitation of hydrophobic functionalized multiwall carbon nanotubes in an aqueous environment. 2012. Journal of Colloid and Interface Science. 368, 115-120.

Desai, C., Meng, X., Yang, D., Wang, X., Akkunuru, V., Mitra, S. 2011. Effect of solvents on stabilization of micro drug particles. Journal of Crystal Growth. 314, 353-358.

Conference Presentations:

Desai, C., Mitra, S., Water pollution from carbon nanoparticles. The Dana Knox Research Show Case, NJIT, Newark, NJ, April 2013.

Desai, C., Mitra, S., Effect of solvents on long term stability of colloidal API suspensions. ISPE NC Annual Meeting, New Brunswick, NJ, April 2013.

Desai, C., Mitra, S., Stable carbon nanotubes (CNTs) as potential water pollutants. 244th ACS National Meeting and Exposition, Philadelphia, PA, August 2012.

Desai, C., Mitra, S., Effect of solvents on stabilization of micro drug particles for effective drug delivery. The 57th Annual New Jersey Academic of Science Meeting, Seton Hall University, South Orange, NJ, April 2012.

Desai, C., Mitra, S., Stable carbon nanotubes (CNTs) as potential water pollutants. The Dana Knox Research Show Case, NJIT, Newark, NJ, April 2012.

Desai, C., Mitra, S., Effect of solvents on stabilization of micro drug particles. 243th ACS National Meeting and Exposition, San Diego, CA, March 2012.

Desai, C., Mitra, S., Water pollution via precipitation of hydrophobic functionalized multiwall carbon nanotubes in an aqueous environment. NJIT GSA Research Day, Newark, NJ, November, 2011.

This Doctoral Degree would not have been possible without some of the most important people in my life. I would like to dedicate this thesis to my father, the Late Ramesh-Chandra Kapadia who was not only my role model but my strength who taught me how to initiate first step towards fulfilling my goal with never giving up attitude. It is dedicated to my mother, Geetaben Kapadia who has been a constant motivational source to me. I am heartily grateful to her for instilling importance of hard work and always being my strength during moments of despair and discouragement.

My gratifying thanks to my wonderful loving husband, Brijesh Desai for his enduring understanding, invaluable patience, and encouragement throughout my journey. A special thanks to my son, Manav who is my joy of life and has grown into 3 wonderful years old in spite of his mother spending so much time away from him working on this dissertation.

Finally thanks to my sisters, niece, nephews, all my friends and family members who endured this long process with their undying love and support.

ACKNOWLEDGMENT

I would like to express my sincere gratitude to my advisor, Dr. Somenath Mitra, for providing invaluable guidance, scholarly inputs, consistent encouragement and opportunities during the course of my doctoral study. I am also very grateful to Dr. Carol A. Venanzi, Dr. Edgardo T. Farinas, Dr. Haidong Huang and Dr. Pradyot Patnaik for their contributions as members of my dissertation committee and providing valuable feedback.

I greatly appreciate the help of, Dr. Marino Xanthos and Ms. Clarisa González-Lenahan, as well as the staff of the Graduate Studies Office and Faculty throughout my study at NJIT. I am immensely grateful to National Science Foundation and National Institute of Environmental Health Sciences (NIEHS) for financial support. My appreciation also goes to the Department of Chemistry and Environmental Science for offering Teaching Assistantship.

Additionally, I would like to thank Dr. Larisa Krishtopa, Dr. Young Pu, Yogesh Gandhi, Gayle Katz and Genti Price for their assistance during my study at NJIT. I also would like to thank my colleagues, Dr. Chutarat Saridara, Dr. Cheng Li, Dr. Yuhong Chen, Dr. Ornthida Sae-Khow, Dr. Xiangxin Meng, Dr. Chaudhery Hussain, Dr. Sagar Roy, Xinbo Cui, Smruti Ragunath, Zheqiong Wu, and Zhiqian Wang for their friendship, collaboration, and exchange of thoughts and ideas. Very special thanks to my friend Dr. Susana Addo Ntim and Dr.Shweta Naik for kind support and help throughout this process. Finally, I would like to take the opportunity to thank my beloved family for their love and support.

TABLE OF CONTENTS

TABLE OF CONTENTS
(Continued)

Chapter **Page**

TABLE OF CONTENTS
(Continued)

LIST OF TABLES

LIST OF FIGURES

LIST OF FIGURES
(Continued)

Figure **Page**

CHAPTER 1

INTRODUCTION

1.1 Objective

Nanotechnology refers to the engineering of functional materials at the atomic, molecular or macromolecular scale (Ebbesen, 1996). Nanoparticles (NPs) are known to have unique size dependent electrical, magnetic, mechanical, optical and chemical properties that make them attractive for various applications (Das et al., 2013; Meyers et al., 2013). Some of the engineered nanomaterials are already found in consumer products such as sporting goods, tires, sunscreens, cosmetics, and electronics, while others will potentially be used in the medical field for diagnosis, imaging, and drug delivery (Kayser et al., 2005; Kostarelos et al., 2005; Hussain et al., 2010; Fan et al., 2011; Fakruddin et al., 2012; Jeyaraj et al., 2013; Sultana et al., 2013). With the emergence of nanotechnology, products containing nanomaterials have grown exponentially and their mass production has become possible. The release of these manufactured nanoparticles into natural aquatic systems is quite expected. The potential impacts of these emerging contaminants on the environment and human health are still uncertain although they are causing growing concern to the community (Ali-Boucetta et al., 2013; David, 2013; Du et al., 2013; Gaiser et al., 2013; O'Shaughnessy, 2013; Popescu et al., 2013; Van Hoecke et al., 2013).

The fate, bioavailability, and exposure risks of these contaminants once released into aquatic systems are directly controlled by their transport behavior in such systems. Compared to bulk particles, micro/nano particles have an extremely high tendency of adhesion and aggregation due to their surface structures and interactions. (Buzea et al., 2007). Environmental exposure, bioavailability, and mobility of NPs in part depend on

their aggregated state and their surface charge therefore it is quite important to control the dispersion/aggregation phenomena of NPs to apply them into functional materials and products. These fundamental characteristics are functions of the aqueous media in which the particles are suspended and dependent on their surface properties and solution chemistry.

The theory of colloid stability is based on the recognition of two forces in any stabilized solution: the electrostatic repulsion which opposes aggregation and an attractive van der Waals force which acts to bind particles together. The theory is known as the DLVO theory after the four scientists – Deryaguin, Landau, Verwey and Overbeek. (Derjaguin and Landau, 1993; Verwey and Overbeek, 1999). The classic DLVO theory of colloidal stability has been universally applied to explain the aggregation and deposition behavior of charged particles in the presence of electrolytes. Many experimental studies on stability of charged nanoparticles of Single wall carbon nanotubes (SWCNTs), Multi wall carbon nanotubes (MWCNTs) and fullerenes have demonstrated their aggregation and deposition behavior to be qualitatively in line with the DLVO theory (Chen et al., 2006; Saleh et al., 2008; Smith et al., 2009).

The interactions between particles control the properties of a colloidal system. For example, adsorbed atoms, especially polymers, can also lead to increases in both flocculation and in repulsion, depending on the nature of the layer and particle. Such stabilization is known as steric stabilization. The purpose of this research is to study the colloidal behavior of water dispersed and organic dispersed materials in aqueous system for various applications. Several systems that throw light on different aspect of this phenomenon are presented. The objectives of this thesis are listed as follows:

- Investigate the stability, mechanisms and aggregation behavior of hydrophobic carbon nanotubes in the aqueous media.
- Carboxylation of nanodiamonds (NDs) and study their dispersion behavior in the aqueous system.
- Investigate the effect of solvents on stabilization of micro drug particles.

1.2 Dispersibility of Colloids

Due to the advent of nanotechnology, many advanced nanoparticles have been developed and their mass production has become increased dramatically in the consumer market. Extensive use of NPs in industry will increase the likelihood of their exposure to the natural environment. For example, nanomaterials such as Carbon Nanotubes (CNTs) and Nanodiamond (NDs) can be released into the environment via wastewater discharge as point source emissions from manufacturing industries (Wiesner et al., 2006). Upon release, they will interact with the aquatic environment and biological species. Depending on the interplay between electrostatic and van der Waals interactions, they may aggregate or persist in aqueous media as homogenous dispersions (Thess et al., 1996). The understanding and effect of such behavior is a key to predicting their deposition, transport, reactivity, and bioavailability in aquatic environments. Literature on aggregation of CNTs and fullerenes has mostly been centered on enhancement of their aqueous solubility, either by dispersing them with surfactant, (Jiang et al., 2003; Lisunova et al., 2006), polymer adsorption (Jung et al., 2004), or by introducing oxygen containing functional groups on the surface through acid treatment (Wang et al., 2005a; Wang et al., 2005b; Chen and Mitra, 2008; Peng et al., 2009). In recent years the number of studies evaluating the aggregation behavior of NPs in the presence of electrolytes has increased significantly, where time-resolved dynamic light scattering (TRDLS), Raman

spectroscopy, zeta-potential measurements, and UV-Visible spectroscopy have been used to investigate the aggregation kinetics of NPs in aqueous (Pavlova-Verevkina et al., 2009; Peng et al., 2009; Smith et al., 2009).

1.3 Electrokinetic Properties of Colloids

Electrokinetic potential is associated with the movement of ionic solutions near charged interfaces. A charged colloidal particle suspended in an electrolyte solution is surrounded by a cloud of counterions which contribute to a set of surface charges and countercharges called the electric double layer. Determination of the detailed structure of the electric double layer is of primary importance in stability issue. This plays an essential role in various interfacial electrical phenomena on the particle surface and in the particle-particle interaction in the colloid suspension. The surface potential on colloid particles is generally difficult to measure. However, the potential near the particle surface called the zeta (ζ) potential is measurable. Zeta potential is the potential difference between the mobile dispersion medium and the stationary phase of the dispersion medium attached to the dispersed particle. The zeta-potential is an important parameter of the electrical double layer and represents a characteristic of electrical properties of solid/liquid interfaces. The zeta-potential is used for observing the behavior of dispersive systems in liquids and is one of the fundamental parameters known to affect stability. It is a measure of the magnitude of the electrostatic or charge repulsion or attraction between particles. Its measurement brings detailed insight into the causes of dispersion, aggregation or flocculation, and can be applied to improve the formulation of dispersions. Zeta potential value can related to the short and long term stability of dispersion. Higher zeta potential value defines the repulsive forces exceeds over to attractive forces and resulting into

stable system. The measurement of zeta potential has important applications in a wide range of industries including; agriculture, ceramics, pharmaceuticals, medicine, mineral processing, electronics, water treatment, etc. Zeta potential has been used to study the stability of MWCNT, fullerene dispersions, and the influence of counterions on their aggregation behavior (Chen et al., 2006; Peng et al., 2009).

Instead of zeta potential, Electrophoretic mobility (EPM) has also been used to measure colloid stability. EPM is the migration of charged colloidal particles through a solution under the influence of an applied electric field. Saleh et al. (2008) studied the electrokinetic properties of MWCNT dispersion in the form of EPM as a function of salt concentration. They observed with increasing the salt concentration made the EPM values of the MWCNTs less negative, as is commonly observed with most colloidal particles in aqueous solutions. The presence of defects on the surface of CNTs in the form of pentagon and heptagon irregularities at their carbon scaffold and also incomplete carbon rings at the end termini make the sidewalls and tube-ends susceptible to oxidation to form carboxyl and hydroxyl functional groups (Hirsch and Vostrowsky, 2005). These functional groups present on the CNT surface accounts for the strong dependence of EPM on solution pH. Smith et al. (2008) investigated the influence of pH on the EPM of oxidized MWCNT in the presence of 64 mM NaCl. The EPM values decreased with increasing pH from pH 3 to 5 with the values remaining fairly stable above pH 6, independent of the electrolyte concentration (Smith et al., 2009). This was consistent with previously reported EPM measurements of oxidized carbon nanotubes (Esumi et al., 1996; Hu et al., 2008). A similar observation was made by Peng et al. while investigating the effect of electrolytes on the stability of oxidized MWCNTs (Peng et al., 2009).

1.4 Aggregation Behavior in Aqueous Media and Effect of Electrolytes

In aqueous system, coagulation of certain colloidal sols is done via addition of electrolytes. For instance, precipitation of SWCNTs, MWCNTs and fullerenes under the influence of different salts often show dependence on the charge on the cations, and in general these nanoparticles have followed the well-established DLVO theory (Derjaguin and Landau, 1993; Verwey and Overbeek, 1999). Where, at low electrolyte concentrations, the aggregation and deposition kinetics increase with electrolyte concentration and at high electrolyte concentration, aggregation is no longer function of concentration and remains constant. It is well-known that the critical coagulation concentration (*ccc*), the minimum concentration of ions necessary to cause rapid coagulation of colloids follows the Schulze-Hardy rule.

$$CCC \sim \left(\frac{1}{z}\right)^{n} \tag{1.1}$$

Where *z* is the valence of the electrolyte counterions. Typically, *n* is 6 in three dimensions (3D) and 9 in two dimensions (Sano et al., 2000). Based on Schuzle-Hardly rule the quantity of the electrolyte which is required to coagulate a definite amount of a colloidal solution depends upon the valency of the ion having a charge opposite to that of the colloidal particles. According to the DLVO theory, the Schulze-Hardy rule results from interplay between van der Waals attraction and electric double-layer repulsion.

Sano et al. were among the first group to investigate the colloidal nature of SWCNTs in electrolyte solutions particularly emphasizing the dependence on the Schulze-Hardy rule (Sano et al., 2001). The state of aggregation of acid-treated SWNTs

was monitored by UV absorbance in solutions containing several inorganic salts. The *ccc* values obtained for Na^{+}, K^{+}, Mg^{2+}, Ca^{3+}, La^{3+} and Ce^{3+} were 37, 26, 0.31, 0.20, 0.050 and 0.052, respectively. A clear inverse relationship between the *ccc* values and the counterion valence *z* was observed, and a plot of the double logarithm of the *ccc* values against valence *z* produced a straight line with a slope of -6 (Sano et al., 2001). It was therefore, concluded that SWCNTs followed the 3D Schulze-Hardy rule. Few studies have quantitatively investigated the colloidal properties of acid-treated, surface-oxidized CNTs. Chen et al. studied CNT aggregate structure in water through light scattering and predicted the fractal dimension of surfactant-modified and acid-treated SWCNTs. They proposed that SWCNTs refluxed in HNO_3 and then sonicated in HNO_3/H_2SO_4 remained stable at neutral pH over a two-week period (Chen et al., 2004; Niyogi et al., 2007). Niyogi et al. studied differences in spectroscopic signatures of SWCNTs at different sodium chloride (NaCl) concentrations to infer about the SWCNT aggregation state (Niyogi et al., 2007). Shieh et al. employed UV-visible spectrophotometry (UV-vis) to show that acid-treated MWCNTs were unstable at pH 0 but increased in aquatic stability between pH 4 and 10, an effect ascribed to the protonation/deprotonation of carboxylic acid groups (Shieh et al., 2007). The oxidation of MWCNTs by HNO_3 or HNO_3/H_2SO_4 has also been investigated by Osswald et al. who observed the formation of negatively charged particles that exhibited an electrophoretic mobility of $\sim$-4 μm s^{-1}cm V^{-1} at neutral pH (Osswald et al., 2007). Giordano et al. have suggested that rod like morphology of CNTs should not follow classical DLVO theory (Giordano et al., 2007).

Saleh et al. (2008) investigated the initial aggregation kinetics of as-prepared MWCNTs using time-resolved dynamic light scattering (TRDLS) (Saleh et al., 2008).

They evaluated the influence of pH, concentration of monovalent (NaCl) and divalent ($CaCl_2$ and $MgCl_2$) salts and the presence of natural organic matter (Suwannee River humic acid, SRHA) on the aggregation kinetics of the MWCNTs. A TRDLS method was used to study the initial aggregation kinetics of MWCNT in the presence of electrolytes and natural organic matter where the hydrodynamic radius of the MWCNTs in the dispersion was measured as function of time over a period of 3 hr to obtain approximately 30% increase in the original hydrodynamic radius of the MWCNTs. The attachment efficiency of the MWCNTs was then determined based on the initial aggregation rate constant k of MWCNTs which is proportional to the initial rate of increase in the hydrodynamic radius, R_h, with time, t, and the inverse of MWCNT concentration N_0 (Chen and Elimelech, 2007):

$$k \propto \frac{1}{N_0}\left(\frac{dR_{h(t)}}{dt}\right)_{t\to 0} \tag{1.2}$$

For MWCNT dispersions with the same nanotube concentration, the attachment efficiency, α, (which is also the inverse of the Fuchs stability ratio, W, commonly used in colloidal stability studies) is obtained by dividing the initial slope of the aggregation profile of a given solution chemistry by the initial slope obtained under favorable (fast) aggregation conditions:

$$\alpha = \frac{\left(\frac{dR_{h(t)}}{dt}\right)_{t\to 0}}{\left(\frac{dR_h(t)}{dt}\right)_{t\to 0,fast}} \quad (1.3)$$

Where the subscript "fast" represents favorable solution conditions, under which rapid, diffusion-limited aggregation takes place. The *ccc* values are then obtained from the intersection of the slow and fast aggregation regimes of the attachment efficiency/electrolyte concentration profile.

Saleh et al. (2008) observed an increase in MWCNT aggregation with increasing salt concentration and counterion valence consistent with the DLVO theory and the Schulze-Hardy rule. The *ccc* value obtained for the monovalent NaCl was 25mM, slightly lower than the value obtained by Sano and coworkers for SWCNT (37mM) (Sano et al., 2001). Although, the reported *ccc* values for other carbon-based nanomaterials, specifically fullerene nanoparticles, are much higher: 85 mM, 160 mM, and 120 mM NaCl (Hong and Elimelech, 1997; Chen et al., 2006; Chen and Elimelech, 2007). For the divalent salts however, the *ccc* values (2.6 mM Ca^{2+} and 1.5 mM Mg^{2+}) were higher than those for SWCNT (0.2 mM Ca^{2+} and 0.3 mM Mg^{2+}) (Sano et al., 2001).

Smith et al. conducted a similar study with oxidized MWCNTs prepared by refluxing pristine MWCNTs in nitric acid, reporting a similar influence of counterion concentration and valence on the observed aggregation behavior (Smith et al., 2009). Their work differed from that of Saleh and coworkers (Saleh et al., 2008) only in the oxidation of the MWCNTs. The influence of natural organic matter was not investigated. The *ccc* values obtained using TRDLS in the presence of Na^{+} and Mg^{2+} and were 93±5

mM and 1.8 mM respectively. While these values were similar to those reported by Saleh and coworkers (Saleh et al., 2008) in the case of the divalent salts, the monovalent NaCl gave a much higher *ccc* value. Peng and coworkers investigated the stability of nitric acid oxidized MWCNTs over a 30 day period in presence of salts by using UV-visible absorption. Their stability investigation showed that during an aging time of 30 days, oxidized CNTs dispersion showed characteristic UV–vis absorbance peak of individual CNTs at 252nm and CNTs concentration reducing to 85% of the initial concentration (Peng et al., 2009). An apparent dependence on counterion valence was observed in agreement with the Schulze-Hardy rule. The minimum concentration of Na^+, K^+, Mg^{2+}, Ca^{2+}, Fe^{3+} and Al^{3+} required to cause precipitation in the MWCNT dispersions were determined based on a previously reported procedure (Peng et al., 2009) and termed precipitation value. The reported values for Na^+, K^+, Mg^{2+}, Ca^{2+}, Fe^{3+} and Al^{3+} were 185 mM, 125 mM, 1.05 mM, 0.55 mM, 0.15 mM, and 0.036 mM, respectively. This value is similar to *ccc* values expect for the Na^+ and their determination may not be as accurate as the procedure for *ccc* determination.

Generally, the *ccc* values obtained for as-prepared CNTs were lower than oxidized ones. Also, the *ccc* values in the presence of divalent and trivalent salts appear to be reproducible across these studies, the values obtained for monovalent salts vary quite a bit (Sano et al., 2001; Saleh et al., 2008; Smith et al., 2009; Ntim et al., 2011).

1.5 Drug Particle Formation and Stability in Aqueous and Nonaqueous Media

Till date, more than 40% of the new chemical entities being generated through drug discovery programs are lipophilic or poorly water-soluble compounds and suffer from poor dissolution rate and lower bioavailability. Sub-micronic colloidal systems are

increasingly used as a mean of addressing such problems in drug formulation (Danhier et al., 2009). The particle size of active pharmaceutical ingredients (API) is the primary variable for controlling the bioavailability of a drug and based on Noyes-Whitney equation (Sanganwar et al., 2010) hydrophobic drugs can be formulated as micro- or nano-particles with high surface area which enhances dissolution rates.

$$\frac{dc}{dt} = kS\ (C_s - C_t) \tag{1.4}$$

Where dc/dt is the rate of dissolution, k is the dissolution rate constant, S is the surface area of the dissolving solid, C_s is the saturation concentration of drug in the diffusion layer and C_t is the concentration of the drug in the dissolution medium at time. Based on this principle, the reduction of particle size leads to a significant increase in the surface area, which in turn can lead to substantial increase in dissolution rate and bioavailability. Smaller the size of the particle, better the physical stability of the dosage form owing to the Brownian motion of the particles in the dispersion. In other respects, it seems that the physical stability of the colloidal systems can often be partly related to the particle mean diameter and size distribution. Hence, particle size of the active agent plays a key role in the physical stability of the drug product. Moreover, the size and distribution of the particles can affect bulk properties, product performance, processability, stability, dose-content uniformity and finally appearance of the end product. The rate of sedimentation, agglomeration, is also affected by particle size. Colloidal systems are multiphase formulations and thus, the designs of stable particle suspensions capable of

long stability constitute a substantial challenge in drug industry and many approaches and technologies have been carried out.

Micro or nano particles can be produced by bottom-up or top-down technologies. Topdown technologies start with bulk material and then break into micro or nano-particles, while bottom-up technologies is to synthesize the material from atomic or molecular species via chemical reactions, allowing the molecules to aggregate to form the solid particles.

1.5.1 Top-down Technologies

Milling and homogenization are the traditional top down methods for size reduction of large quantities of particulate materials. No harsh solvents are used in these processes and high loading of the materials can be achieved. In fact, these high energy processes produces a lot of heat which makes thermo labile materials to process (Rasenack and Müller, 2002b). The biggest problem with top down approach is the imperfection of surface structure and significant crystallographic damage to the processed patterns. These imperfections would have a significant impact on the device design and fabrication of nanostructures and nanomaterials. Regardless of the defects produced by top down approach, they will continue to play an important role in the synthesis of nano/micro structures which leads to the bulk production of nano/micro materials.

1.5.2 Bottom-up Technologies

The bottom-up approach plays an important role in the fabrication and processing of nanomaterials. In recent years, bottom-up processes such as emulsification and precipitation methods have emerged as methods for the synthesis of submicron or micro-particles from the liquids. The colloidal dispersion is a good example of bottom up

approach in the synthesis of nano particles. Bottom-up processed can be carried out at ambient temperatures, and therefore heat sensitive materials can be processed easily. Nanostructures with less defects, more homogenous chemical composition, and better short and long range ordering can be achieved via bottom up processes. One of the main disadvantages of these methods is the need to remove excess stabilizer and solvent by appropriate techniques.

1.5.3 Anti-solvent Precipitation Method

Precipitation methods such as antisolvent precipitation have been utilized for many years and are widely used in chemical and pharmaceutical industry for preparation of submicron particles for drug delivery (Zimmermann et al., 2007; Xia et al., 2010), for the production of pigments and dye stuffs, in mineral industry for the separation and purification of ores as well as preparation for other nanoparticles (Bilati et al., 2005; Kakran et al., 2012). Precipitation processes are of utmost importance in environmental technology for the purification of waste water from heavy metals and for the recovery of resource material. Precipitation method is the crystallization of sparingly soluble substances. Typically, a poorly water soluble material is first dissolved in an organic solvent and the solution is mixed with a miscible anti-solvent (Figure 1.1). The ultrasonic agitation was used to assist particle precipitation during mixing. Precipitation processes that form particles directly may provide more control of particle size distribution and morphology. Researchers have reported sonication assisted anti-solvent precipitation for the formation of submicron and micro-particles of hydrophobic drugs for drug delivery. (Meng et al., 2009; Desai et al., 2010; Zhu et al., 2011). Anti-solvent precipitation of organic dispersed carbon nanotube has also been carried out to study fate and transport of

such materials in aqueous system (Desai et al., 2012). The stabilization of these suspensions is of great importance for both controlling the particle size and developing manufacturing processes.

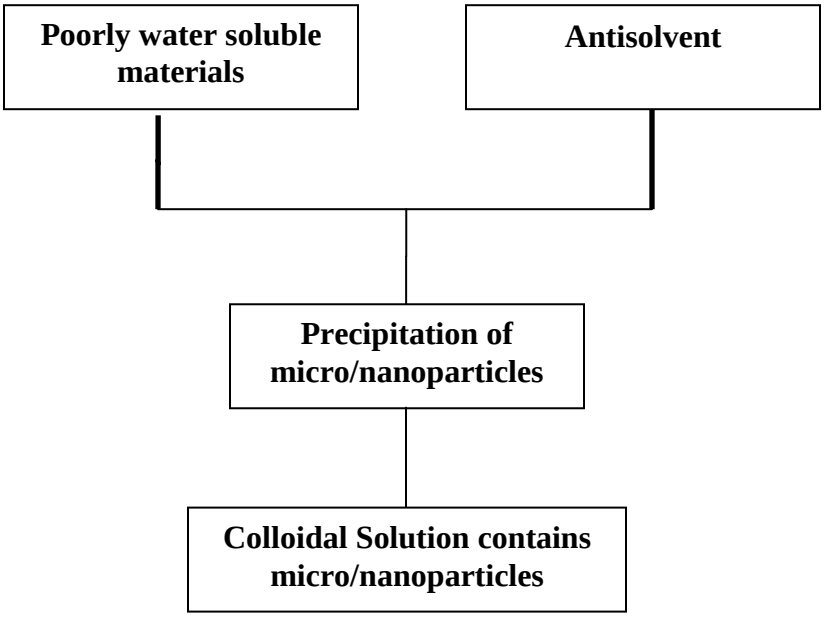

Figure 1.1 Approach for anti-solvent precipitation.

In precipitation method a chemical reaction produces precipitation of micro/nano particles via nucleation and growth. The mechanism of antisolvent precipitation is shown in Figure 1.2. Precipitation generally involves the simultaneous and rapid occurrences of primary processes in the presence of other secondary processes. The primary processes are mixing of the solute molecules at molecular scale via nucleation and growth. The nucleation rate depends on the degree of supersaturation and is the driving force for the precipitation. High supersaturation leads to higher nucleation rate which can produce homogenous or heterogenous systems (Mersmann, 1999). Nucleation occurs when a critical number of molecules join together to form nuclei. Nucleation and growth

continue to occur simultaneously while the supersaturation exists. Supersaturation can be highly sensitive to the rate at which the solvent and antisolvent are mixed, compared to the induction time for nucleation to occur and therefore, the mixing time, $\tau_{mix,}$ must be small compare to the process time, $\tau_{flash,}$ in order to obtain a homogenous mixture.

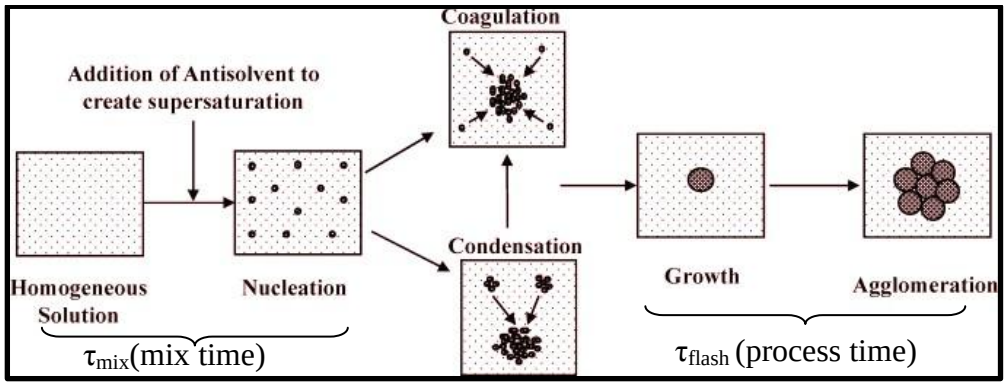

Figure 1.2 Mechanism of anti-solvent precipitation.

Secondary processes are aggregation, ageing and ripening of the molecules. The coagulation process usually occurs after particle precipitation which results in particle collision and formation of bigger particles. Agglomeration describes the tendency of small particles in a liquid suspension to coalesce into larger aggregates. The nucleated primary particles remain in the submicron range and are subject to colloidal interactions which depend on the properties of the particles and the liquid. These interactions may be attractive or repulsive and consequently phenomena-like particle aggregation, particle flocculation or colloidal stability are governing the formation and structure of the final product particles.

1.5.4 Improving the Dispersion Stability of Nanoparticles

Nanoparticles are known to have high tendency of adhesion and aggregation due to their surface structures and surface interactions. Thus, it is quite important to develop techniques to control the dispersion/aggregation of NPs to apply them into various applications. And in particular, to control the stability of dispersion of NPs in an organic media is still a challenging issue. Surface modification is one of the mostly accepted methods to improve the dispersion stability of NPs to overcome such challenges. The three main approaches that have been used to solubilizes NPs are; surfactant-based solubilization (Islam et al., 2003) non-covalent wrapping/adsorption, where soluble polymers have been wrapped (Lin et al., 2003), and covalent functionalization involving chemical modification of the NPs surface (Wang et al., 2005b; Chen and Mitra, 2008; Peng et al., 2009).

1.6 Functionalization of Nanocarbons and Their Stability

The family of nanocarbons is quite diverse including well-known materials such as carbon nanotubes, fullerenes, nano-carbon black, and nanodiamonds. Carbon-based nanoparticles have attracted significant attention due to their unique physical, chemical, and electrical properties and have potential application in various fields. Applications of the nano-carbon materials mainly depend on the degree of the dispersion of the nano-carbon materials into the related medium, such as aqueous phase, organic phase, or polymer materials. Their low solubility, poor wettability and bad dispersibility in common solvents and solid matrices have limited their processing and applications. For example, pristine CNTs and NDs are rather inert to chemical attack and difficult to disperse or dissolve in water and other organic solvents. Some level of functionalization

is therefore, required prior to their utilization in real-world applications. Thus, the attempt to achieve wettable/processable nanocarbons by functionalization has attracted increasing attention in both scientific and industrial communities and various nanomaterials have been functionalized using diverse techniques (Esumi et al., 1996). Several routes/methods to functionalization have been reported (Kuzmany et al., 2004) but non-covalent wrapping/adsorption (Hu et al., 2006; Zhang et al., 2006; Zhang et al., 2012) and covalent tethering (Valentini et al., 2005; Grujicic et al., 2007; Chang and Liu, 2009; Basiuk et al., 2012) are the two main routes which have been extensively investigated. As a typical kind of nanomaterials, this thesis will focus on chemical functionalization of CNTs and NDs. Surface functionalization techniques include tethering, such as, amidation (Huang et al., 2002) and sidewall carboxylic acid functionalization (Peng et al., 2009) in particular.

1.6.1 Carbon Nanotube Functionalization

The unique properties of CNT such as high aspect ratio, extremely high mechanical strength but ultra-light, high thermal conductivity, high stability, and rich electronic properties make it desirable for different applications. Carbon nanotubes in their pristine form are generally chemically stable and insoluble in water or organic solvents. For most of the real world applications, nanotubes require the preparation of homogenous mixtures of CNTs with different organic, inorganic, and polymeric materials. Some level of functionalization is therefore necessary, such as changing some of the graphite properties to make nanotubes soluble in different media, or attaching certain molecules to their sidewalls without significantly changing their physical/electronic properties for future utilization of modified nanotubes. All functionalization methods of CNTs can be divided

into two major group endohedral (Functionalization from inside) or exohedral (chemical functionalization from outside). Endohedral functionalization of the CNTs involves the filling of the tubes with atoms or small molecules. Exohedral functionalization can be achieved via covalent functionalization by attaching functional groups to the nanotube ends or defects and sidewall functionalization or via noncovalent functionalization via wrapping nanotubes by polymers.

Covalent functionalization of CNTs is based on covalent linkage of functional entities, either at the end caps of the tubes or sidewalls. This can involve either a direct covalent functionalization where a change in hybridization from sp^2 to sp^3 and a simultaneous loss of conjugation occurs, or defect functionalization where chemical transformations occur at defect sites already present at the open ends or the sidewalls, or pentagon and heptagon irregularities in the graphene framework. Oxygenated sites, formed through the oxidative purification, have also been considered as defects. Non-covalent functionalization on the other hand involves supramolecular complexation using various adsorption forces, such as van der Waals' and π-stacking interactions (Hirsch and Vostrowsky, 2005). The CNTs have also been functionalized by attaching biological molecules, such as, lipids, proteins, and biotins (Petrov et al., 2004). These may even mimic biological functions, such as, protein adsorption or binding to DNA/drug molecules (Chen et al., 2001; Martínez et al., 2009). Polymers, such as, polyaminobenzoic sulfonic acid (PABS), polyimide, and polyvinyl alcohol (PVA) and polyvinyl pyrrolidone (PVP) (O'Connell et al., 2001; Ntim et al., 2011) have also been used to functionalize CNTs via wrapping or chemical bonding.

1.6.2 Nanodiamond Functionalization

Another class of carbon based nanomaterials which possess unique physical and chemical properties are NDs. NDs are first identified in the 1960's in Soviet Union (Shenderova et al., 2002a) are now reaching world-wide attention due to their unique properties and easily modified surfaces. NDs are known to be for their extreme hardness, chemical inertness, high thermal conductivities, wide optical transparency and other unique properties. NDs have been synthesized via detonation technique, laser ablation (Yang et al., 1998), high-energy ball milling of high-pressure high-temperature (HPHT) diamond microcrystals (Boudou et al., 2009), plasma-assisted chemical vapour deposition (CVD) (Frenklach et al., 1991) autoclave synthesis from supercritical fluids (Gogotsi et al., 1996), chlorination of carbides (Welz et al., 2003), ion irradiation of graphite (Daulton et al., 2001), electron irradiation of carbon onions (Banhart and Ajayan, 1996) and ultrasound cavitation (Galimov et al., 2004). Among these, NDs produced by detonation method have made the ND powder commercially available in ton quantities which enabled many engineering applications. They are most commonly synthesized through mixtures of trinitrotoluene (TNT) and 1, 3, 5-trinitro-1, 3, 5-*s*-triazine (RDX), in a negative oxygen balance chamber.

The DND has the smallest particle sizes among particulate synthetic diamonds, mainly in the range of 4 to 5 nm. Compared to other carbon based nanomaterials NDs consist of a three-layered structure such as a core (sp^3 atoms) which includes 70-90 % carbon atoms and has a size of 40-60 A^o, an intermediate shell of amorphous carbon (sp^2 atoms) around the shell which consists 10-30 % carbon atoms and a surface layer which contains heteroatoms in addition to carbon. The number of heteroatoms may be quite

large, about 10 % of the particle mass and most of them are oxygen atoms (Krüger et al., 2005). DND materials have a wide variety of surface groups that are naturally present on the particles' surface due to detonation and post-detonation procedures (Kulakova, 2004). As a result, DNDs are unique among their larger carbon classification since they may contain a multifaceted collection of chemical groups, often including hydroxyl, carboxylic acids, esters, ethers, lactones, amines and more (Shenderova and Ciftan Hens, 2010).

Such various functional groups can be used for covalent functionalization as well as can create a barrier to attach certain groups on the DND surface. The surface-modification of DND can be achieved via combining the physical properties of DND crystals and chemical properties of organic functional groups attached to the DND surface by using same approaches which have been used to functionalize CNTs. Although, some unique properties of DND such as low electric conductivity, surface heterogeneity due to presence of several oxygen containing groups and low solubility in different solvents make DND functionalization quite challenging in compare to CNTs.

CHAPTER 2

ANTISOLVENT PRECIPITATION OF HYDROPHOBIC FUNCTIONALIZED MULTIWALL CARBON NANOTUBES IN AQEUOUS ENVIRONMENT

2.1 Introduction

The industrial production of carbon Nanotubes (CNTs) has increased quite dramatically in recent years, because they have found a variety of new commercial applications. These applications increase the likelihood of environmental contamination. Pristine CNTs tend to settle out of aqueous media into solid phases such as river sediments. On the other hand, hydrophilic, functionalized CNTs (f-CNTs) may persist in aquatic media/environment and can serve as water pollutants. Therefore, the understanding of their fate in aqueous media is of great importance.

Numerous approaches have been employed to disperse CNTs in aqueous as well as nonaqueous media. The most common approaches include the use of surfactants (Sun et al., 2002), covalent functionalization of CNT surface (M. F. Islam, 2003; Kang et al., 2006) and noncovalent interactions with different polymers including DNA (Daniel et al., 2007; Yang et al., 2007; Noguchi et al., 2008; Kharisov et al., 2009). The f-CNTs can be classified as hydrophilic and hydrophobic, where the former is water dispersible and the latter is soluble in organic solvents. Examples of water dispersible CNTs are carboxylated and hydroxylated CNTs, while the latter includes aminated and other hydrophobic functionalities.

Understanding the colloidal behavior of CNT dispersions can be useful in studying their fate and transport in the aquatic environment and several publications have

addressed this issue (Saleh et al., 2008; Smith et al., 2009). Aggregation kinetics of CNTs has been studied using time-resolved dynamic light scattering (TRDLS), Raman spectroscopy, Zeta potential measurements, and UV-Visible spectroscopy (Chiang et al., 2001; Peng et al., 2009). Aggregation of carboxylated CNTs in the presence of different salts has demonstrated that (Manivannan et al., 2009) precipitation is dependent on the charge on the cations, and in general these nanoparticles have followed the well-established DLVO theory (Derjaguin and Landau, 1993; Verwey and Overbeek, 1999). While the water dispersibility of covalently functionalized CNTs originates from electrostatic repulsive forces between negative surface charges, polymer wrapped CNTs are stabilized sterically by the presence of the hydrophilic polymer on the surface. Studies have shown that the aggregation behavior of such polymer wrapped CNTs is quite different from covalently functionalized CNTs (Ntim et al., 2011).

The interest in water dispersible CNTs as water pollutants has grown, but the behavior of hydrophobic, organic soluble f-CNTs has not been addressed. Under normal circumstances, one would expect these f-CNTs to settle out of an aqueous media. Unexpectedly, waste water from manufacturing plants could potentially carry dispersed hydrophobic f-CNTs in presence of organic solvents into water resources leading to their antisolvent precipitation. Such precipitation occurs due to supersaturation caused by mixing of a solution and an antisolvent (Zhang et al., 2009). Precipitation occurs instantaneously by rapid desolvation of the solute and under the right circumstances could form stable colloids. Accordingly, it is conceivable that under appropriate conditions, these f-CNTs may be stabilized in aqueous media where they will serve as water pollutants. The precipitation and stabilization of hydrophobic f-CNTs in aqueous

media is yet to be studied, and it is conceivable that it will be affected by various parameters such as the type of solvent and the presence of other electrolytes. Moreover, the dispersion mechanisms are expected to be quite different from the hydrophilic f-CNTs studied before (Ntim et al., 2011), and it is not known if the conventional approaches such as the DLVO theory would be applicable here.

This chapter describes the possibility of antisolvent precipitation of hydrophobic, organic soluble f-CNTs where water acts as an antisolvent. Particularly focus was on to stydy their aggregation behavior and mechanisms in the aqueous media, and see if they are significantly different from their hydrophilic counterparts.

2.2 Preparation of F-CNTs

Carboxylate multiwalled carbon nanotubes (MWCNT-COOH) and Octadecylamine functionalized multiwalled carbon nanotubes (MWCNT-ODA) were functionalized in a Microwave Accelerated Reaction System (Mode: CEM Mars) fitted with internal temperature and pressure controls according to an experimental procedures previously published by (Chen and Mitra, 2008). A pre-weighed amount of purified MWCNT was treated with a mixture of concentrated H_2SO_4 and HNO_3 solution by applying them to microwave radiation at 140 °C for 20 min. This led to the formation of carboxylic groups on the surface leading to high aqueous dispersibility. The resulting solid was filtered through a 10μm membrane filter, washed with water to a neutral pH and dried under vacuum at 80 °C to a constant weight.

The MWCNT-COOH was used as the starting material to synthesize organic dispersible MWCNTs. In reaction vessel pre-weighed amount of MWCNT-COOH was mixed with thionyl chloride ($SOCl_2$) and Dimethylformamide (DMF). The reaction

vessel was subjected to microwave radiation around 70 °C for 20 min. The final suspension was filtered and washed with Tetrahydrofuran (THF) until there was no brown color in the solution. These solids were dried in a vacuum oven at room temperature for 12 h and it converted to MWCNT-COCl product. After that, this product mixed with pre-weighed octadecylamine (ODA) and heated in the microwave reaction vessel at 120 °C for 10 min. The reaction vessel was placed at room temperature and the excess ODA was removed by washing with hot ethanol several times. The remaining solids were filtered. The unreacted ODA was washed with dichloromethane. The resultant black residue (MWCNT-ODA) was dried at room temperature under vacuum to obtain final product. This product is soluble in THF, Ethanol, Acetone and Acetonitrile (ACN).

2.2.1 Characterization of the MWCNT-ODA

The materials were characterized by scanning electron microscope (SEM), thermo gravimetric analysis (TGA), and Fourier Transform Infrared spectroscopy (FTIR). SEM data was collected on a LEO 1530 VP Scanning Electron Microscope equipped with an energy-dispersive X-ray analyzer. TGA was performed using a Pyris 1TGA from Perkin-Elmer Inc. from 30 °C to 900 °C under a flow of air at 10mL/min, at a heating rate 10 °C per min. FTIR measurements were carried out in purified KBr pellets using a Perkin-Elmer (Spectrum One) instrument.

2.2.2 Dispersibility Studies

A 1000 mg l^{-1} stock solution of MWCNT-ODA was prepared by sonicating pre-weighed amount of the MWCNT-ODA in THF, ethanol, acetone, ACN solvents. Various concentrations were then prepared by diluting the stock solution by ultrasonication. For

dispersibility study, solvent/water ratio was altered by changing the amount of water. The hydrodynamic diameter was measured using a Malvern Instrument (Zetasizernano ZS90). A 400 mM stock solution of sodium chloride (NaCl) was prepared by dissolving weighed amount of salt in MilliQ water. Dilutions were carried out as needed. Aggregation data was collected using 1mg L^{-1} dispersion of the MWCNT-ODA in the presence of electrolyte solutions whose concentration ranged between 10 and 200 mM. The measurements were performed for a time period ranging from 120 s to 3 h. It should be noted that the Dynamic Light Scattering (DLS) system used here models hydrodynamic radius based on the diffusion of the particles, and the latter depends on viscosity. With the exception of ethanol, the viscosity of rest of the solvents were between (0.38 and 0.55 cP), while ethanol was 1.1 cP. Since the maximum concentration of solvent was no more than 12%, the effect of viscosity is considered to be negligible, and it is assumed that the particle sizes are acceptable on a relative basis.

2.3 Results and Discussion

2.3.1 Characterization

SEM images of original MWCNT and MWCNT-ODA are presented in a and 2.1b. These show that the nanotube structures were maintained without visible tube damage during functionalization process.

The IR spectrum (Figure 2.2 b) confirmed the presence of functional groups in the MWCNT- ODA. The peak around 1573 cm^{-1} was assigned to the C=C stretching of the carbon skeleton. The sharp peak around 1639 cm^{-1} was attributed to stretching vibrations of the amide group. The peak around 1735 cm^{-1} was attributed to the stretching vibration

of C=O group. The sharp peaks at 2847 cm^{-1} and 2921 cm^{-1} were attributed to the stretching vibration of alkyl chain from ODA (Figure 2.2b). A FTIR spectrum confirms the successful grafting of ODA on carboxylate carbon nanotubes.

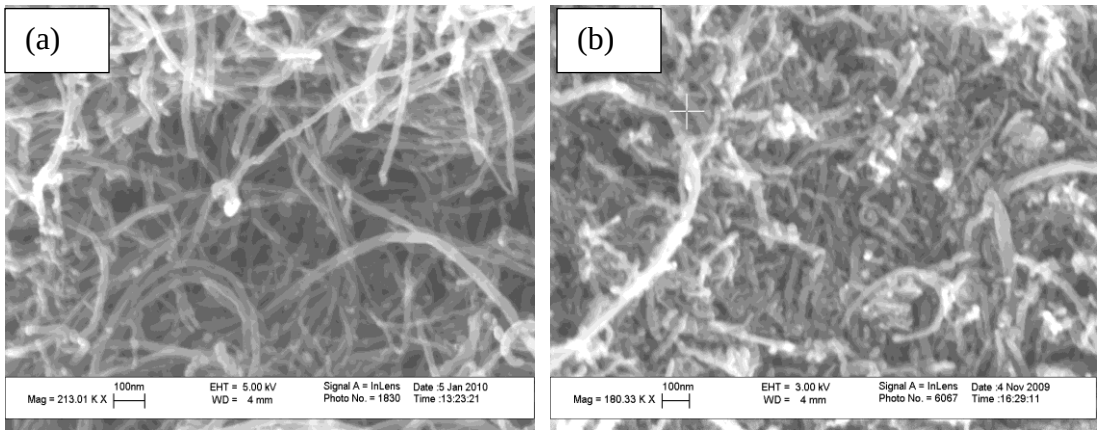

Figure 2.1 SEM images of (a) MWCNT (b) MWCNT- ODA.

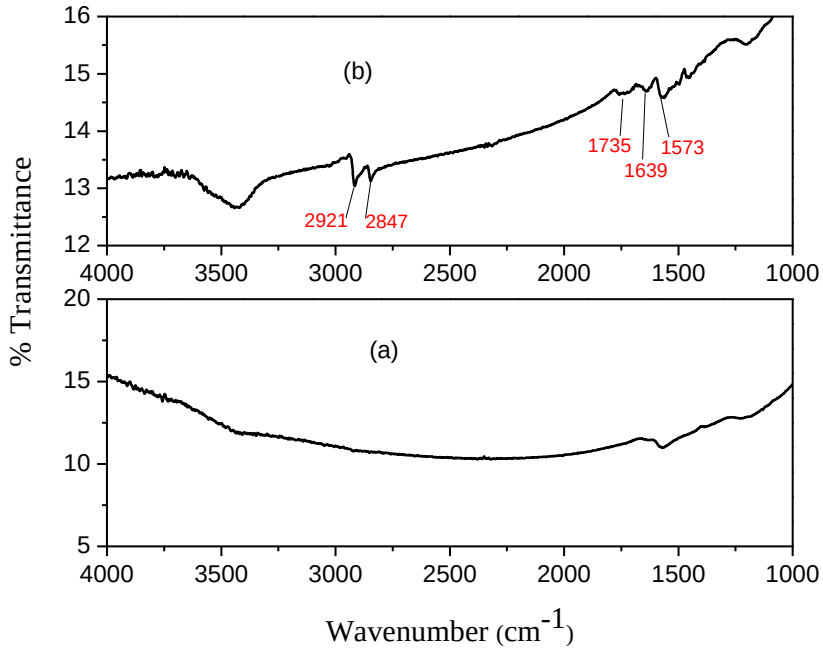

Figure 2.2 FTIR spectra of (a) purified CNT and (b) MWCNT-ODA.

The TGA was used to quantify the degree of functionalization and is presented in Figure 2.3. The weight loss in the 100 ^{o}C to 400 ^{o}C in MWCNT-ODA profile was attributed to the decomposition of ODA group. The ODA accounted for 19.3% of the total weight in the MWCNT-ODA.

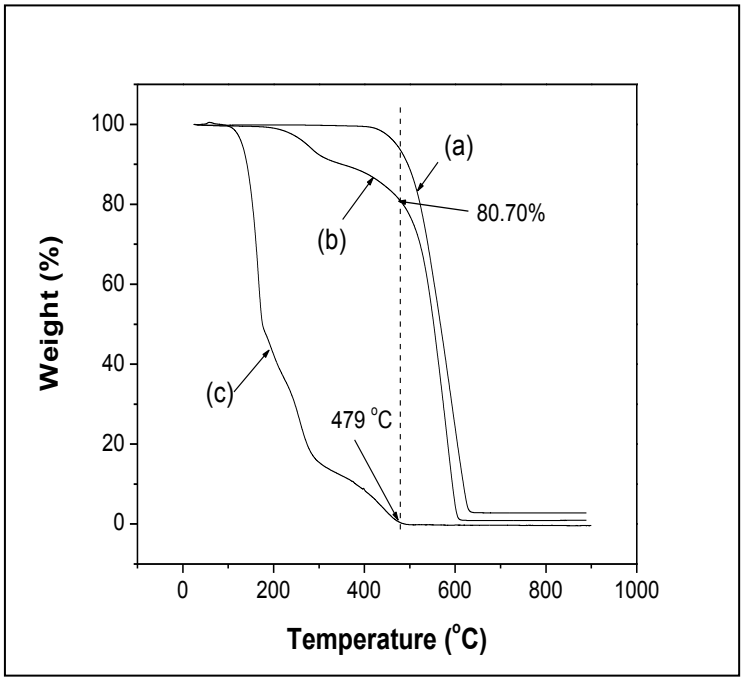

Figure 2.3 TGA of (a) purified MWCNT, (b) MWCNT-ODA (c) pure ODA.

2.3.2 Antisolvent Precipitation of MWCNT-ODA in Aqueous Media

The MWCNT-ODA solutions were prepared in THF, ethanol, acetone, ACN and toluene. Among the solvents studied, the MWCNT-ODA had the least solubility in toluene, and it was not used for further investigations. The presence of an organic solvent is a key factor because it affects miscibility in water as well as the degree of supersaturation. Here, the effect of solvents on the antisolvent precipitation was studied. When MWCNT-ODA solution (in an organic solvent) was mixed with water, antisolvent precipitation of MWCNT-ODA occurred but the nanotubes remained dispersed. Without addition of

oppositely charged molecules a colloidal suspension could stay stable for long periods of time. This demonstrates that when discharged into the aquatic environment, the organic soluble CNTs can form stable dispersions and serve as potential water pollutants. Photographs of MWCNT-ODA dissolved in THF (a), antisolvent precipitated (c) and precipitated MWCNT-ODA in presence of NaCl (d) are shown in Figure 2.4. The MWCNT-ODA was not soluble in water (Figure 2.4 b).

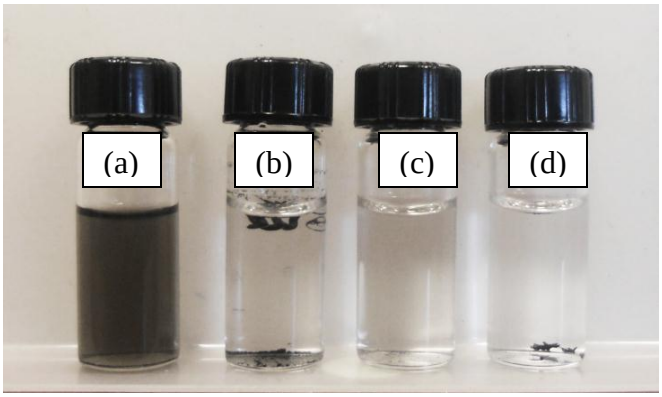

Figure 2.4 Photographs of (a) MWCNT-ODA dispersed in THF Solvent (10ppm); (b) precipitation of MWCNT- ODA in water; (c) dispersed MWCNT-ODA after antisolvent precipitation; (d) partial precipitation of dispersed MWCNT-ODA after addition of NaCl.

Figure 2.5 shows the particle size distribution of stable MWCNT-ODA colloid in aqueous medium and in the presence of different solvents. The dispersibility of MWCNT-ODA showed similar trend in acetone and ethanol but the behavior was markedly different in THF and ACN. When water was added as an antisolvent, it reduced the solubility of MWCNT-ODA and increased the supersaturation to form particles. The level of supersaturation depended upon two factors, namely the concentration of dissolved species and the solvent–antisolvent ratio (Dong et al., 2011). These factors influenced the nucleation and growth rates of the particles. The particle size distribution

in presence of ethanol and acetone did not appear to be affected by the solvent/water ratio; but THF appeared to have significant effect. The difference in dispersibility in presence of THF may be attributed to polarity and hydrogen bonding of the solvent, which are presented in Table 2.1.

Table 2.1 Hansen Parameters for Solvents

Solvents	Polar Component (δp)	Hydrogen Bond(δH)
THF	5.7	8
Ethanol	18.8	19.4
Acetone	10.4	7
Acetonitrile	18	6.1

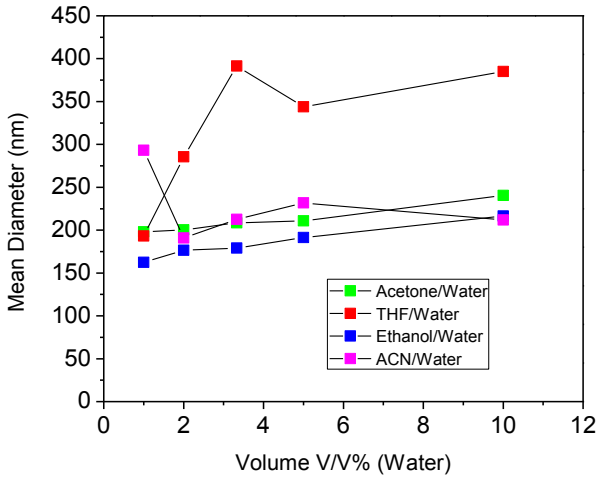

Figure 2.5 Particle size distribution of MWCNT-ODA in solvent/water mixtures containing 10 ppm of MWCNT-ODA in four solvents.

Based on the Hansen solubility parameters presented here, THF had the lowest value of δp (polar component) and was least miscible in water (Ausman et al., 2000). The miscibility of the solvent and antisolvent is an important criterion in antisolvent methods and it is well known that when the solubility in water decreases faster aggregation and sedimentation occur (Lee et al., 2007). As a result, the agglomeration of the MWCNT-

ODA was maximum in the THF/water system. On the other hand, ACN/water system showed a different trend at higher concentration. When the concentration increased, the supersaturation degree increased and more MWCNT-ODA precipitated which led to the larger particle size.

2.3.3 Long Term Stability of MWCNT-ODA

The stability in terms of particle size distribution of the precipitated MWCNT-ODA as a function of time is shown in Figure 2.6. These measurements were carried out at lower concentrations. The trend was similar in the concentration range of 1.66 to 10 ppm, and only these two concentrations are presented here for brevity. It was observed that MWCNT-ODA dispersion in four water/solvent mixtures was stable over the 24 hour measurement period. Mean particle diameters ranged from 170 to 400 nm, and were different for four solvent/water mixtures.

The main driving force for antisolvent precipitation process is the supersaturation generated by different solubility of a solute in the solvent and antisolvent. Typically, when solute concentration is increased, more nuclei are produced in the solvent–nonsolvent interface resulting in the inefficient mixing of solvent and antisolvent and therefore larger particles are formed (Tóth et al., 2005). This was observed in presence of ACN, where larger particles were formed at higher concentration. Nonetheless, the trend was opposite for the THF/water, acetone/water and ethanol/water systems. Here the particle size appeared to decrease with increasing MWCNT-ODA concentrations. In these three systems supersaturation occurred at lower concentrations of MWCNT-ODA leading to the formation of larger particles. However, at higher concentration of

MWCNT-ODA some of these large particles may have settled out of the solution, and the dispersed particles showed a smaller particle size distribution (Meng et al., 2009).

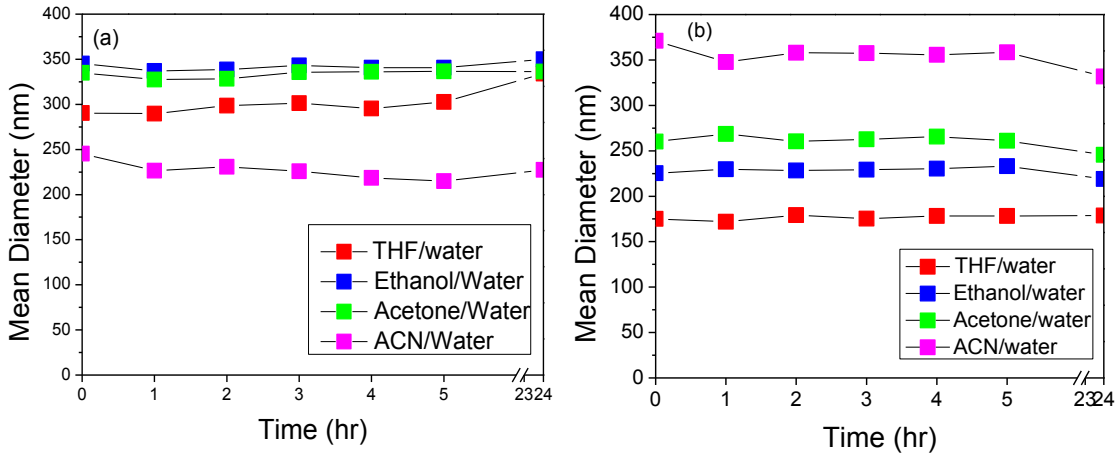

Figure 2.6 Particle size distribution of MWCNT-ODA in (a) 1.66 ppm concentration of MWCNT-ODA and in (b) 10 ppm concentration as a function of time.

2.3.4 Effect of Salt on the Stability of MWCNT-ODA Dispersion

Figure 2.4 (d) shows the precipitation of MWCNT-ODA on the addition of sodium chloride (NaCl). It can be seen that, the presence of NaCl led to further agglomeration and the particle size of MWCNT-ODA precipitates increased in all solvent/water systems. This is seen in Figure 2.7, which shows that the particle size increased with salt concentrations. With the exception of the ethanol/water system, the observed increase in particle size was similar to the behavior of PVP wrapped multiwall carbon nanotubes in the presence of sodium chloride, where size increase was gradual even at high salt concentration. It was opposite to the behavior of carboxylate MWCNTs where a drastic increase in particle sizes was observed with increasing salt concentration (Addo Ntim et al., 2011). This increase was maximum for the ethanol/water and THF/water systems. While acetone/water and ACN/water systems showed relatively lower agglomeration.

Ethanol has the highest hydrogen bonding and also the highest electron pair donor ability compared to the other solvents (Ausman et al., 2000), and hence higher solubility with water (Table 2.1). As a result, when electrolyte was added to the ethanol dispersion of MWCNT-ODA, the agglomeration was maximum. On the other hand THF has least polarity (Table 2.1) and hence least miscibility with water. And so, when MWCNT-ODA added to THF/water system higher supersaturation and faster crystal growth occurred in presence of electrolyte and which leads to agglomeration of the particles.

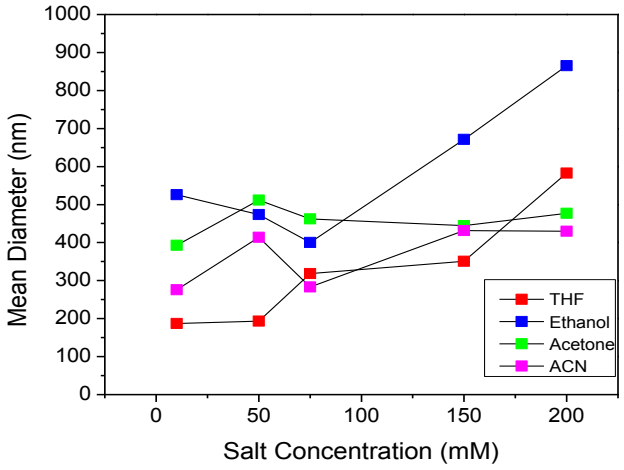

Figure 2.7 Particle size distribution of MWCNT-ODA in solvent/water mixtures as a function of salt concentration.

The effect of salt species in a solvent/water mixture depends on the interaction of the disperse molecules with the solvent, the binding of water molecules to solvent, and changes in the hydrogen bonding interaction due to the added salt. The addition of an electrolyte also changes the hydrogen-bonded structure of water. The addition of salt into solvent/water mixture dispersion changed the association and could disrupt the highly oriented water molecules surrounding the solvent as well as disperse molecule leading to

change in the system (Addo Ntim et al., 2011). The positively charged metal ion from the salt can also neutralize the surface charge on MWCNT-ODA, and compress the double layer of the dispersed nanotubes. This could reduce the electrostatic repulsive forces which were present due to the delocalization of electrons in amide group and led to precipitation (Chiang et al., 2001; Peng et al., 2009; Smith et al., 2009).

2.3.5 Aggregation of MWCNT-ODA in Presence of Electrolyte

The aggregation kinetics of MWCNT-ODA in the presence of NaCl for four solvent/water systems were examined using time resolved dynamic light scattering method. Aggregation kinetics was measured by monitoring the time-dependent increase in hydrodynamic radius (r_h). The initial aggregation rate constant (k) of MWCNTs is proportional to the initial rate of increase in the hydrodynamic radius (rh) and inverse of MWCNT-ODA concentration (n_0). The attachment efficiency (α) which is the reciprocal of stability ratio 1/W for suspensions were computed by using equation 2.1

$$\alpha = \frac{\left(\frac{dR_{h(t)}}{dt}\right)_{t\to 0}}{\left(\frac{dR_h(t)}{dt}\right)_{t\to 0,fast}} \tag{2.1}$$

Where $\left(\frac{dR_{h(t)}}{dt}\right)_{t\to 0}$ and $\left(\frac{dR_h(t)}{dt}\right)_{t\to 0,fast}$ represent the slow and fast aggregation regimes respectively. The fast aggregation also represents the favorable aggregation regime. Figure 2.8 shows the attachment efficiency, which is a measure of the ratio of the initial slope of the aggregation profile in a given solution system to the slope obtained under fast aggregation conditions.

According to DLVO theory, in the low concentration region, an increase in attachment efficiency is normally observed with increase in salt concentration, while at high concentrations, the attachment efficiency is no longer a function of concentration and remains constant. This is due to the decrease in the electrostatic repulsion. According to Figure 2.8, the attachment efficiency increased linearly with time during the initial stages of aggregation. However, for all the solvent/water systems, it did not reach a steady state. This was quite different from what has been previously reported for water dispersible CNTs (Addo Ntim et al., 2011). Thus it was evident that unlike hydrophilic CNTs (Addo Ntim et al., 2011), the antisolvent precipitated hydrophobic CNTs did not follow the DLVO theory.

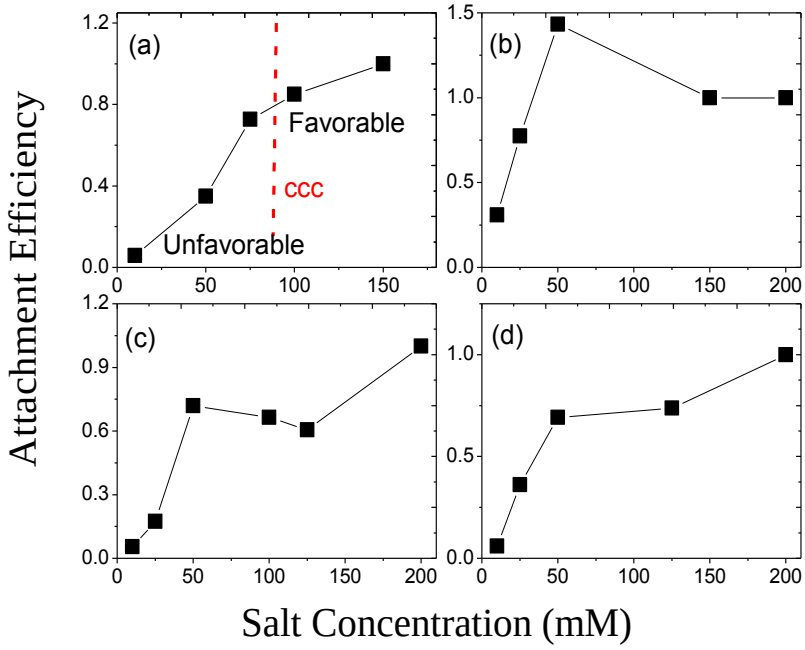

Figure 2.8 Attachment efficiency of MWCNT-ODA in (a) THF/water (b) ethanol/water(c) acetone/water (d) ACN/water in presence of electrolyte.

All the four systems showed different behavior in the higher salt concentration regions and the critical coagulation concentration (CCC) could not be estimated according to the DLVO theory. However, if the point where the kinetic curve changes slope is taken as a pseudo CCC value, then they would be 90 mM, 55 mM, 60 mM, and 30 mM for THF/water, ethanol/water, acetone/water and ACN/water respectively. These pseudo CCC values were significantly lower than CCC values observed for highly hydrophilic carboxylate and polymer wrapped MWCNT reported before (Smith et al., 2009; Addo Ntim et al., 2011). The CCC values represent the minimum salt concentration required to form agglomeration of the particles in the system. Higher CCC values represent the shorter settling rate. Based on these values, the THF/water system showed better long term stability in presence of electrolyte.

2.4 Conclusions

The precipitation and stabilization of hydrophobic, organic soluble F-CNTs in aqueous media was studied, where water acted as an anti-solvent for their precipitation. MWCNT-ODA served as the model F-CNT and results with THF, acetone, acetonitrile and ethanol suggest that the organic soluble F-CNTs can form stable dispersions in water where the solvent affects the dispersibility. Particle aggregation increased with the addition of electrolytes, with THF and ethanol showing the maximum effect and typical particle sizes ranged from 170 to 400 nm. The understanding of the aggregation behavior of these F-CNTs can be useful in predicting their fate and transport in aquatic environments.

It is interesting to note that unlike hydrophilic CNTs, the anti-solvent precipitated hydrophobic CNTs did not follow the DLVO theory. The four systems studied here showed different behavior and the CCC values could not be estimated according to the

DLVO theory. A pseudo CCC value was defined as the point where the kinetic curves changed slope, and they were found to be 90, 55, 60, and 30 mM for THF/water, ethanol/water, acetone/water and ACN/water respectively. These pseudo CCC values were significantly lower than CCC values observed for highly hydrophilic f-CNTs reported before. Among the solvents studied, the THF/water system showed the best long term stability in presence of electrolytes.

CHAPTER 3

MICROWAVE INDUCED CARBOXYLATION OF NANODIAMONDS

3.1 INTRODUCTION

The relatively inexpensive large scale production of Nanodiamonds (NDs) by a detonation synthesis process has made them commercially viable for a broad range of applications (Dolmatov et al., 2004; Kruger et al., 2006; Dolmatov, 2007; Kharisov et al., 2010; Mochalin et al., 2012). NDs have tetrahedral network structures, small size (5-10 nm) (Greiner et al., 1988), large grain boundary and density (Zapol et al., 2002) and low to negative electron affinity (He et al., 2000)which makes them attractive for diverse applications ranging from additives to drug delivery (Dolmatov, 2001; Wang et al., 2003; Baidakova and Vul, 2007; Osawa, 2008; Williams et al., 2008; Burleson et al., 2009). The optical transparency and wide band gap make NDs semiconductor material with a wide range of electronic applications (Turner et al., 2009), while the combination with high mechanical strength, stiffness, light weight and low coefficient of friction makes them suitable for the fabrication of structural composites (Choi et al., 1996; Chong et al., 2006; Maitra et al., 2009). NDs comprise of a diamond core (sp^3), middle core (sp^{2+x}) and a graphitized core (sp^2) (Nagata et al., 2010). The applications of most nanocarbons including NDs have been limited because of inherent incompatibility with solvents, polymers and other matrices.

The NDs are resistant to chemical attack and some level of functionalization is needed for their processing, especially in solution phase. Functionalization of Detonation

nanodiamonds (DND) has been studied based on the physical properties of the diamond core and chemical properties of surface functional groups. The outer surface contains many dangling bonds that facilitate various covalent bondings. Several techniques have been developed for surface modification for NDs including the mechanical disruption of the bundles, non-covalent (Yu et al., 2005; Nguyen et al., 2007) and covalent methods (Maitra et al., 2008). Much of the efforts have involved usage of conventional chemical techniques such as milling (Osawa, 2008; Gour, 2010) sonication and refluxing (Kulakova, 2004; Krüger et al., 2005; Li et al., 2006; Gour, 2010).

Many of these reactions were required to be carried out over long periods of time. For example, for carboxylation, the reaction mixture was typically refluxed with strong acids or oxidizing agents for 10-50 hr (Kulakova, 2004; Kruger et al., 2006; Li et al., 2006; Jee and Lee, 2009). One of the first modification techniques developed by Shenderova and his group used radical based reactions under wet chemical treatments where the hydrogen atom was removed to create a free radical species for binding carboxylic acids (Shenderova et al., 2002b). Ushizawa and his group used gas phase functionalization method based on reaction with chlorine, fluorine and hydrogen gas phase to generate surface functional groups(Ushizawa et al., 2002). Tu and his group used thermally annealed NDs with CCl_4/Ar mixtures to generate surface functional groups (Tu et al., 2006). Non-covalent functionalization of NDs has been carried out by attaching surfactants, peptides, proteins and polymers on the NDs surface (Loktev et al., 1991; Huang and Chang, 2004; Spitsyn et al., 2006; Zhu et al., 2007; Schrand et al., 2009; Neitzel et al., 2011). Most of the above mentioned methods are tedious, time

consuming and are having some drawbacks and hence it is important to develop techniques for rapid chemical functionalization of NDs.

Reactions under the microwave radiation are somewhat different, faster and have been exploited in a variety of organic synthesis procedures with reported advantages of higher yields and selectivity (Caddick, 1995; Bogdal et al., 2003; Wiesbrock et al., 2004). There is also the reported microwave effect which is known to alter chemical activation parameters (Hens et al., 2008). Microwave assisted functionalization of MWCNTs and SWCNTs via carboxylation, amidation, sulfonation and other reactions has been reported by Chen et al. and Wang et al. has shown some excellent advantages such as reduction of reaction times from hours to minutes (Wang et al., 2005b; Chen and Mitra, 2008).

Due to a large number of surface defects and a large surface/volume ratio, DNDs tend to exhibit higher surface reactivity compared to other carbon nanostructures such as CNTs. In fact, the graphene structures in CNTs have high electrical conductivity which makes them highly microwave active, while the NDs are semiconductors and their low electric conductivity (0.2987×10^{-12} s/cm) reduces their microwave activity. Consequently, mainly the sp^2 bonded surface carbon atoms are the major contributor towards microwave heating. This puts NDs in a unique position, at one hand they are more reactive, but the other hand they are less microwave active. However, the possibility of microwave induced functionalization which could lead to the shortening of reaction time, and higher degree of functionalization could provide major advantages.

This chapter focuses on the microwave assisted functionalization of DND, with the possibility of higher dispersion in an aqueous matrix. Of Particular interest is carboxylation, which is the basic first step for the synthesis of other functional groups.

3.2 Carboxylation of DNDs

DNDs were functionalized in a Microwave Accelerated Reaction System (Mode: CEM Mars) fitted with internal temperature and pressure controls. The 100 mL reaction chamber was lined with Teflon PFA® with an operating range of 0∼200 ^{0}C and 0∼200 psi. The as-received nanodiamonds were referred as DND and were treated with 1:1 70% nitric acid and 97% sulfuric acid in microwave reaction vessels. Various power and time and reaction times were tested, and the carboxylated NDs were referred to as DND-COOH. The resulting solid was filtered through a 10μm membrane filter, washed with water to a neutral pH and dried under vacuum at 80 °C to a constant weight.

3.2.1 Characterization of DNDs

The materials were characterized by scanning electron microscope (SEM), X-ray diffraction (XRD) and Fourier Transform Infrared spectroscopy (FTIR). SEM measurements were made by applying a drop of the ND dispersions on the sample holder and data was collected on a LEO 1530 VP Scanning Electron Microscope equipped with an energy-dispersive X-ray (EDX) analyzer. The X-ray diffraction measurements were carried out by scanning the 2θ range from 5 degree to 149 degree using CuKα (λ=0.15406 nm) radiation as the light source. FTIR measurements were carried out in purified KBr pellets using a Perkin-Elmer (Spectrum One) instrument.

3.2.2 Particle Size and Zeta Potential Measurements

A 100 mg/L stock solution of DNDs and DND-COOH were prepared by sonicating pre-weighed amount of the DND materials in MilliQ water. From that various concentration were prepared to study dependency of zeta potential and particle size on sample concentration. Samples were sonicated for 30 minutes and measurements were carried

out on Malvern Instrument (Zetasizernano ZS90). Solubility was measured by dispersing 2 mg of both ND materials in 20 ml of selected solvents by sonicating for 2 hrs. The top 15ml of the solution, containing most dissolved samples, were decanted and the solvent evaporated. The obtained residue was weighed and the solubility was calculated in mg/L.

3.3 Results and Discussion

Unlike the CNTs and other carbon nanomaterials, DNDs are composed of three layers, a diamond core (sp^3) which includes 70-90% of carbon atoms, an intermediate core which may include 10-30% amorphous carbon atoms and a chemically active surface layer. For example, an individual ND grain measuring 4.3 nm in diameter is reported to consist of about 7200 carbon atoms, of which nearly 1100 are on the surface (Shenderova et al., 2002b). Surface of NDs prepared by detonation process are known to contain a wide variety of functional groups and in this case contained significant amount of oxygen. The surface functionalities and oxygen content were confirmed using FTIR and EDX and are presented below.

Microwave heating occurs either by dipolar polarization or via conduction or joule heating ((Thostenson and Chou, 1999; Motshekga et al., 2012). During the microwaved induced liquid phase oxidation, the ionic and dipolar molecules such as water undergo collision induced heating caused by rapid vibration. Graphite, carbon nanotubes and other graphene and amorphous carbon structures are known to be strong absorbers of microwave, heat via conduction and serve as superheated centers that are extremely reactive. Subsequently, microwave induced CNT functionalization has shown fast kinetics and high degree of functionalization (Wang et al., 2005b; Wang et al., 2006; Chen and Mitra, 2008). For the DNDs studied here, the sp^2 carbon atoms are strong

microwave absorber, whereas the core sp^3 is relatively less microwave active. As a result, it was anticipated that the DNDs would behave differently than other nanocarbons such as nanotubes and graphite. Different reaction temperatures and oxidation times were tested for microwave induced oxidation of P-NDs. Most of them led to negative results implying that the functionalization did not occur or the level was unsatisfactory. For example, CNTs are known to functionalize within 3 to 20 min functionalization (Wang et al., 2005b; Wang et al., 2006; Chen and Mitra, 2008), but that was not possible with the DNDs. Carboxylation was achieved at 95% of a total of 1600 watts power, the temperature setting of 75 ^{o}C and reaction time of 1 hr. The reaction time was significantly longer than that encountered for CNTs. This is attributed to the low microwave absorption by the DNDs.

3.3.1 Characterization

Figure 3.2 shows the SEM images of DNDs (Figure 3.2 a) and DND-COOH (Figure 3.2 b) respectively. From the figures it can be seen that no significant microstructural or morphological changes were observed on the particles after acid treatment. SEM images also revealed that DND-COOH showed no detectable damage to its structure. The primary diamond particles look spherical and partly agglomerated in both DND dispersions. Oxidation led to some color change, which can be seen in Figure 3.1.

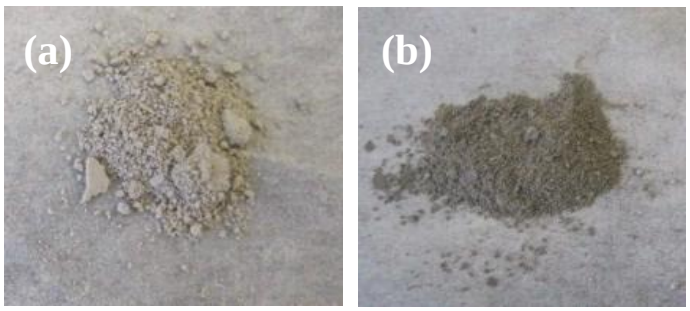

Figure 3.1 Photographs of (c) DND and (d) DND-COOH.

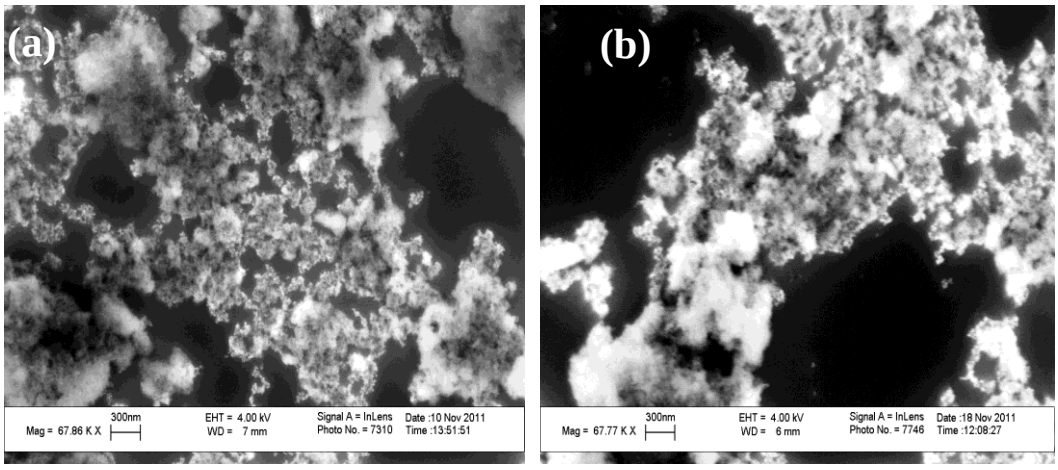

Figure 3.2 SEM images of (a) DND (b) DND-COOH

Elemental compositions were measured using Energy Dispersive X-ray analysis (EDX). The elemental compositions are presented in Table 3.1. It was noted that weight percent of oxygen (O) atom increased significantly (nearly tripled) after acid treatment, implying carboxylic group formation on the DND surface.Figure 3.3 shows the XRD pattern of both DND samples. As shown in Figure 3.3, the diffraction pattern of the DND have three broader peaks at 2θ=44, 73 and 92^{o} corresponding to the (111), (220) and (311) cubic diamond planes, which demonstrates that the DND crystal was cubic. Figure 3.3 (b) shows that DND maintain their crystal structure after the acid treatment and was unaffected by the carboxylation.

Table 3.1 Elemental Composition of DND Compounds

Elements	DND		DND-COOH	
	Weight%	Atomic %	Weight%	Atomic %
Carbon (C)	94.90	96.12	85.33	88.57
Oxygen (O)	5.10	3.9	14.67	11.43

Note: Commercial NDs and Carboxylated NDs were referred as DND and DND-COOH respectively.

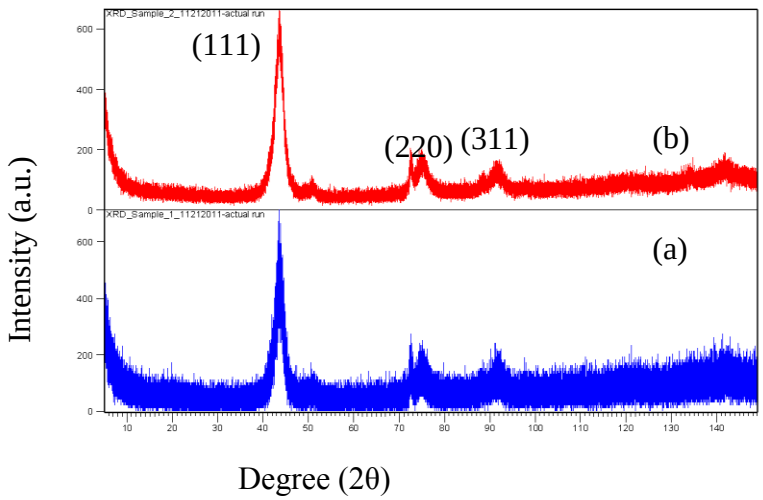

Figure 3.3 Powder X-ray diffraction spectra of (a) DND (b) DND-COOH.

The surface chemistries of NDs with and without strong acid treatments were characterized and compared by FTIR. Oxygen-containing surface groups such as hydroxyl, carboxylic, lactones, ketones and ethers are usually present on the nanodiamond particles surface and can be observed in Figure 3.3 (a). Figure 3.3 (b) shows the FTIR spectra of the DND-COOH. For the commercial DND powder, the main features in the spectrum are related to C-H (2923 cm^{-1} stretch and 1382 cm^{-1} bend), O-H and N-H (1630 cm^{-1}), COC (1107 cm^{-1}) and O-H vibrations (3422 cm^{-1} stretch and 1630 cm^{-1} bend), which have been assigned to surface functional groups such as aldehydes, esters, alcohols, acids and amines. For the DND-COOH powder, there are almost the same IR adsorptions as those of DND except COC peak which has shifted from 1107 to 1117 cm^{-1}. The significant peak appearance at 1728 cm^{-1} indicates the presence of carboxylic group on the DND surface confirms the conversions of original functional groups like ketones, aldehydes, alcohols and esters into carboxylic acids.

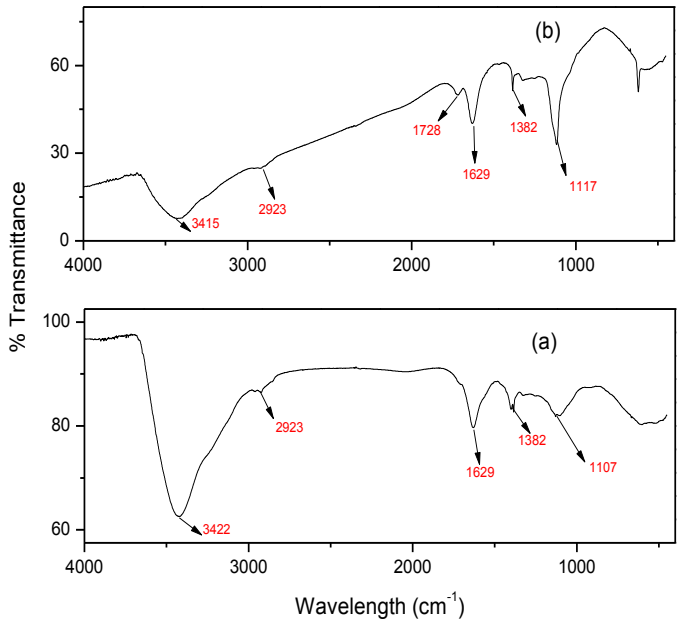

Figure 3.4 FTIR spectra of (a) DND and (b) DND-COOH.

3.3.2 Colloidal Behavior of DND Dispersions

Dynamic Light Scattering (DLS) was used to study the colloidal behavior of DNDs in aqueous as well as organic media. DNDs are known to agglomerate with the formation of primary and secondary structures due to the presence of a large number of functional groups. It is well known that primary DND particles are 4 to 5 nm in diameter, but they tend to agglomerate and form larger aggregates (Aleksenskiĭ et al., 1999). Due to the high specific surface area and electrostatic interactions, the DNDs are likely to aggregate into larger clusters, which are affected by carboxylation. However, the nanodiamond core which was unaffected by the carboxylation did not participate in this agglomeration process. The carboxylation reduced agglomeration in the aqueous phase. The particle size distribution was measured after 30 min of sonication. Table 3.2 shows the particle size and solubility values for DND dispersions. From the data it can be observed that

particle size of the agglomerates was significantly lower after carboxylation leading to better dispersion. This was also true when Tetrahydrofuran (THF) and Dimethyl Sulfoxide (DMSO) were used as solvents, with the effects being most dramatic for THF. The DND had low solubility (or dispersibility) in all the solvents. Carboxylation improved solubility in water as well as in organic solvents and that can be observed in Table 3.2.

Table 3.2 Particle Size and Solubility of DND Materials

	Particle Size (nm)		Solubility (mg/L)	
Solvents	DND	DND-COOH	DND	DND-COOH
Water	347.4	302.1	66.66	93.33
THF	1199	403.5	106.66	173.33
DMSO	582.1	486.7	200	226.66

The colloidal stability was also quantified by zeta potential measurements. The dependence of zeta potential and particle size on sample concentration is presented in Figure 3.5 (a) and (b). An increase in the absolute value of the zeta potential by several mV was observed as the sample concentration was increased and this was attributed to the dissociating surface groups on the ND surface. The results indicate that dissociation process was concentration dependent. The C-NDs consistently showed higher zeta potential. Figure 3.5(b) shows the particle size of both ND dispersions at different concentrations and it was observed that carboxylation reduced particle agglomeration.

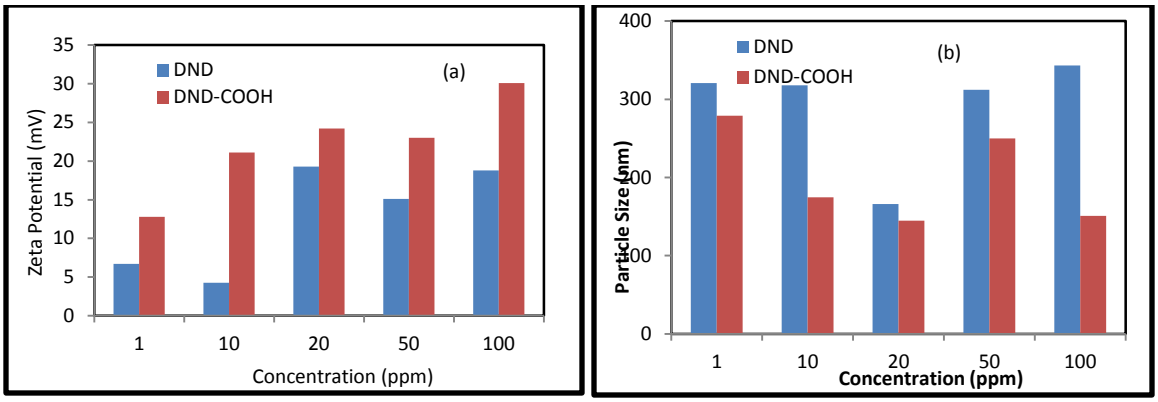

Figure 3.5 (a) Zeta potential (b) particle size as a function of DND concentration in water.

3.4 Conclusions

A fast, cost-effective and environmentally-friendly microwave-assisted method for the functionalization of DND is presented. FTIR measurements confirmed the presence of carboxylic group on the DND surface. The DND-COOH formed stable dispersion in aqueous as well as organic solvents, and showed higher solubility in water, THF and DMSO. The solubility, dispersibility and stability improved by the functionalization, and the oxidized DND containing –COOH could be used for further functionalization via diverse synthetic routes.

CHAPTER 4

AGGREGATION BEHAVIOR OF NANODIAMONDS AND THEIR FUNCTIONALIZED ANALOG IN AQUEOUS ENVIRONMENT

4.1 Introduction

Nanodiamonds produced by detonation of explosives under an oxygen-deficient atmosphere are becoming an increasingly important class of materials (Van Thiel and Ree, 1987; Greiner et al., 1988; Shenderova et al., 2002a). The DNDs have tetrahedral network structures, and the detonation DNDs comprise of a diamond core (sp^3), a middle core (sp^{2+x}) and a graphitized outer core (sp^2) that is often partially oxidized. Large grain boundary density, low to negative electron affinity and small size of 5 to 10 nm makes them attractive to a variety of applications. The DNDs have found many applications in high precision polishing (Yu. Dolmatov, 2001), nanofluidic for thermal conduct polymer composites (Maitra et al., 2009), wear- resistant surface coatings (Chu et al., 2010), and biological applications (Gruen et al., 2005; Grichko et al., 2008).

The industrial production of DND has increased quite dramatically in recent years and the widespread use of this nanomaterial can be a source of environmental contamination. Another important consideration is that several routes have been explored to modify DND surface which help to achieve stable suspensions in polar and nonpolar solvents and allow other functionalities such as biomolecules to be attached (Krüger et al., 2005; Li et al., 2006; Shenderova et al., 2007; Schrand et al., 2009; Meyers et al., 2013). Due to their small size, the DNDs are relatively stable in aqueous media, while their functionalized analogs may be even more stable. Consequently, these DNDs have the potential to contaminate water resources and be highly bioavailable. Considering

everything, there is a need to develop an understanding of the fate and transport of these DNDs in aqueous media.

Aggregation behavior of other nanoparticles such as carbon nanotubes (CNTs) and fullerene has been studied using time-resolved dynamic light scattering (TRDLS), Raman spectroscopy, zeta potential measurements, and UV–Visible spectroscopy (Chiang et al., 2001; Peng et al., 2009). Precipitation of the carboxylated CNTs and also the fullerene under the influence of different salts has shown that (Manivannan et al., 2009; Smith et al., 2009) precipitation is dependent on the charge on the cations and in general these nanoparticles have followed the well-established Derjaguin–Landau–Verwey–Overbeek (DLVO) theory (Derjaguin and Landau, 1993; Verwey and Overbeek, 1999). The stability and aggregation kinetics of DNDs is yet to be studied and this chapter focuses mainly on the colloidal behavior of DND and its carboxylated analogs (DND-COOH).

DND was functionalized in a Microwave Accelerated Reaction System (Mode: CEM Mars) fitted with internal temperature and pressure controls using a method published before (Desai and Mitra, 2013) which was briefly described in Chapter 3. Same materials were used further, to study aggregation kinetic and dispersibility in presence of electrolytes.

4.2 Preparation of DND Dispersions

Stock solutions (100 mg L^{-1}) of DND and DND-COOH were prepared by sonicating pre-weighed amounts of the DNDs in MilliQ water. Various concentrations of DND solutions used in this study were then prepared by diluting the stock solution by ultrasonication. Stock solutions (400 mM) of sodium chloride (NaCl) and magnesium chloride ($MgCl_2$)

were prepared by dissolving weighed amounts of salt in MilliQ water and dilution was carried out on as needed basis.

The stability of 50 mg l^{-1} dispersions of both DNDs over a 24 h period was determined in the presence of 25 mM solutions of NaCl and $MgCl_2$ using fluorescence at 753.2 nm. This was measured at 0, 1, 2, 4, 6, and 24 h. Their dispersion stability indices were determined as a function of their fluorescence absorbance at 0 hr (Elimelech et al., 1998; Ntim et al., 2011).

The hydrodynamic diameter of 1 mg L^{-1} DND dispersions was measured as a function of salt concentration at 25 ^{o}C using dynamic light scattering (Beckman Coulter N_4 Plus submicron particle size analyzer, operated at 90^{o} detector angle), where the salt concentrations ranged from 10 to 200 mM. The Zeta potential of the DND dispersions was measured at a concentration of 5 mg L^{-1} at 25 ^{o}C using a Malvern Instrument (Zetasizernano ZS90). Measurements were made in MilliQ water and as a function of electrolyte concentration. Aggregation data for DND dispersions was collected using 1 mg L^{-1} dispersions of DND and DND-COOH in the presence of electrolyte solutions whose concentrations ranged from 10 to 200 mM. The measurements were performed for a time period ranging from 90s to 2.5 h.

4.3 Results and Discussion

4.3.1 Particle size and Zeta potential Measurements

Figure 4.1 (a) and (b) shows the particle size distribution of DND and DND-COOH in water as a function of salt concentration. As salt concentration was increased, agglomeration of the particles was observed which led to larger particle size. The DND

surface is characterized by surface heterogeneity where post synthesis processes lead to the formation of several oxygen containing chemical functional groups such as hydroxyl, carboxylic, lactones, ketones and ethers [Burleson et al. 2009]. On the other hand, functionalization process increased the uniformity of the DND surface, and the electrostatic repulsive forces between the DND-COOH groups may lead to increased stability in water. Adding salt to a colloidal suspension caused the double layer to shrink which led to agglomeration. It is interesting to note that in the case of both DNDs, particle size increased rapidly (almost three times) with the addition of as little as 10 mM of salt, and the increase was gradual at high salt concentrations (Figure 4.1). The rate of aggregation was much faster compared to what has been reported before for dispersed CNTs, where the rapid increase in agglomeration was observed only with the addition of 100 mM of salt (Ntim et al., 2011). Also, in case of CNTs, particle size increased quite dramatic (nearly four times) in presence of divalent salts as compared to the monovalent salts for CNTs and fullerenes (Kayser et al., 2005; Ntim et al., 2011) which was not the case for DNDs studied here.

Zeta potential values for both DND and DND-COOH at different salt concentrations were compared and are presented in Figure 4.2. Both showed relatively high zeta potential, and in the absence of any electrolytes, the zeta potential of the DND-COOH was higher than DNDs. The high zeta potential was attributed to the presence of nonpolar carbonaceous species on the DND surface, which improved with further carboxylation, and led to higher colloidal stability for the latter. Addition of salt however resulted in rapid drop in zeta potential and the values for both types of DNDs were similar. In general, for the two DNDs studied here, the effect of the monovalent and

divalent salt on zeta potential was not significantly different, this was unlike what has been reported for CNTs and fullerenes (Kayser et al., 2005; Hussain et al., 2010).

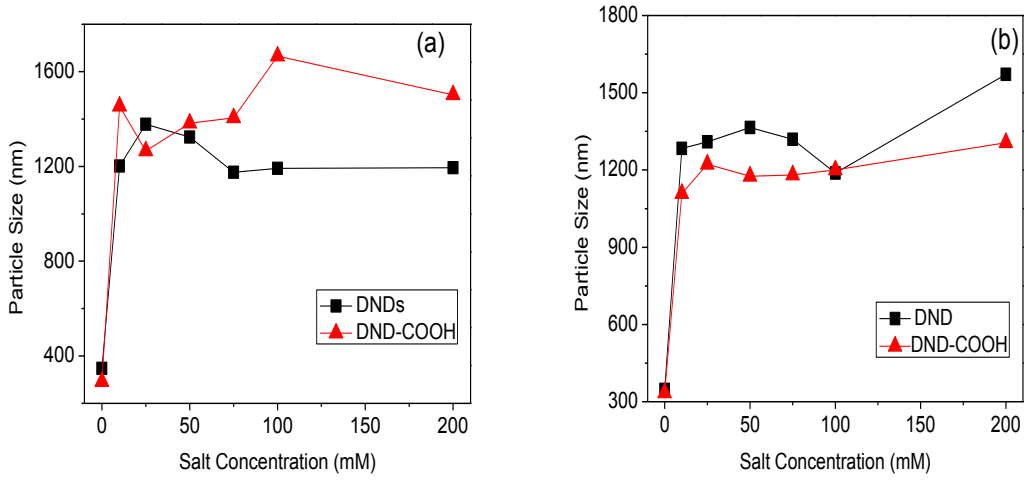

Figure 4.1 Particle size distribution of DND and DND-COOH in presence of (a) NaCl and (b) $MgCl_2$.

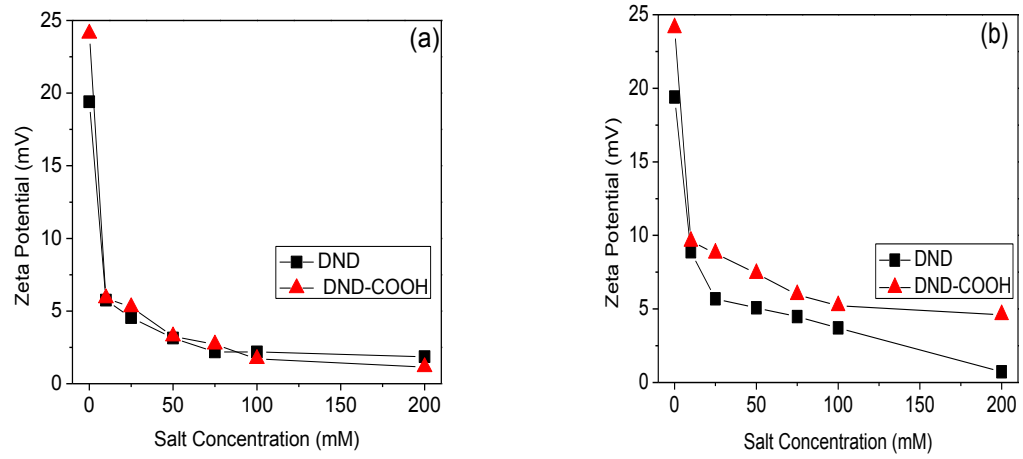

Figure 4.2 Zeta Potential of DND and DND-COOH in the presence of (a) NaCl and (b) $MgCl_2$.

4.3.2 Aggregation and Long Term Stability Study of DNDs

Time-resolved dynamic light scattering was used to investigate the initial aggregation kinetics of both DND dispersions. Aggregation kinetics was measured by monitoring the

time-dependent increase in hydrodynamic radius (r_h). The initial rate of change in particle size (r_h) is proportional to initial aggregation rate constant (kn_o) where k is the initial aggregation rate constant and n_o is the initial concentration of the DND dispersions. The attachment efficiency (α) known as the inverse stability ratio (1/W) is used to quantify the aggregation kinetics of colloidal systems and computed by using Equation 2.1.

The attachment efficiencies at different electrolyte concentrations is a measure of the ratio of the slopes obtained under different solution conditions by the slope obtained under favorable (fast) aggregation conditions are shown in Figure 4.3. The terms with subscript "fast" refer to favorable (nonrepulsive) aggregation conditions. The graph shows the attachment efficiencies of the DND and DND-COOH in NaCl and $MgCl_2$ as a function of salt concentration. Distinct unfavorable and favorable aggregation kinetics regimes demarcated by the critical coagulation concentration (CCC) (Figure 4.3) were observed. In the presence of electrolytes, both DND nanoparticles exhibit classical aggregation behavior, which can be explained by the Derjaguin-Landau-Verwey-Overbeek (DLVO) theory. At low electrolyte concentrations, particles have higher electrostatic repulsions resulting in unfavorable aggregation (slow aggregation). When the electrolyte concentrations approaches or exceed the critical coagulation concentration (CCC), attractive van der Waals forces dominate between the nanoparticles which lead to faster aggregation. Hence, at low ionic strengths, increase in attachment efficiency was observed. At high concentrations, the attachment efficiency was no longer a function of concentration and remained constant. This was similar to what had been reported previously for MWCNT-COOH, fullerene, C60 particles. (Elimelech et al., 1998; Saleh et al., 2008; Chen and Elimelech, 2009).

The CCC values were estimated from the plot of the attachment efficiencies against the salt concentration which shows the slow and fast aggregation regimes (Figure 4.3).The CCC values were obtained from the intersection of the interpolated lines through the slow and fast regimes.

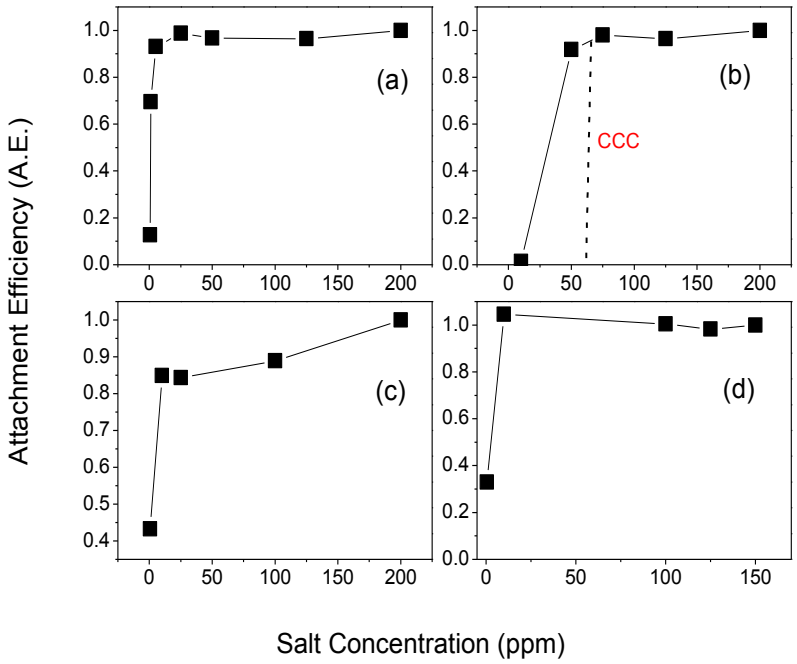

Figure 4.3 Attachment Efficiency of (a) DNDs in NaCl (b) DND-COOH in NaCl (C) DNDs in $MgCl_2$ and (d) DND-COOH in $MgCl_2$.

The estimated value of CCC for DND in presence of NaCl was 21 mM, while that for DND-COOH was 51 mM. Higher CCC values for DND-COOH implies better stability in presence of electrolytes. The CCC values for the DNDs were similar to those reported for MWCNTs (25 mM) [Saleh et al. 2008], slightly lower than that for SWCNT (37mM) (Hussain et al., 2010; Fan et al., 2011) and much lower than fullerenes (80 to 160 mm) (Kayser et al., 2005; Kostarelos et al., 2005) . On the other hand, much higher CCC values have been reported for carboxylated MWCNTs, which have ranged from 95

to 185 mM (Peng et al., 2009; Smith et al., 2009; Ntim et al., 2011). The estimated CCC values in presence of divalent salt ($MgCl_2$) were 10 mM for DND and 2 mM for DND-COOH. The difference between NaCl and $MgCl_2$ for both DNDs was quite apparent and was in line with the Schulze-Hardy Rule. The CCC values in presence of $MgCl_2$ for the DNDs appear to be somewhat higher than what has been reported for SWNTs and MWCNTs, which range from 0.3 to 1.8 mM (Fan et al., 2011), while a higher CCC value of 8.0 mM has been reported for fullerenes in presence of $MgCl_2$ (O'Shaughnessy, 2013).

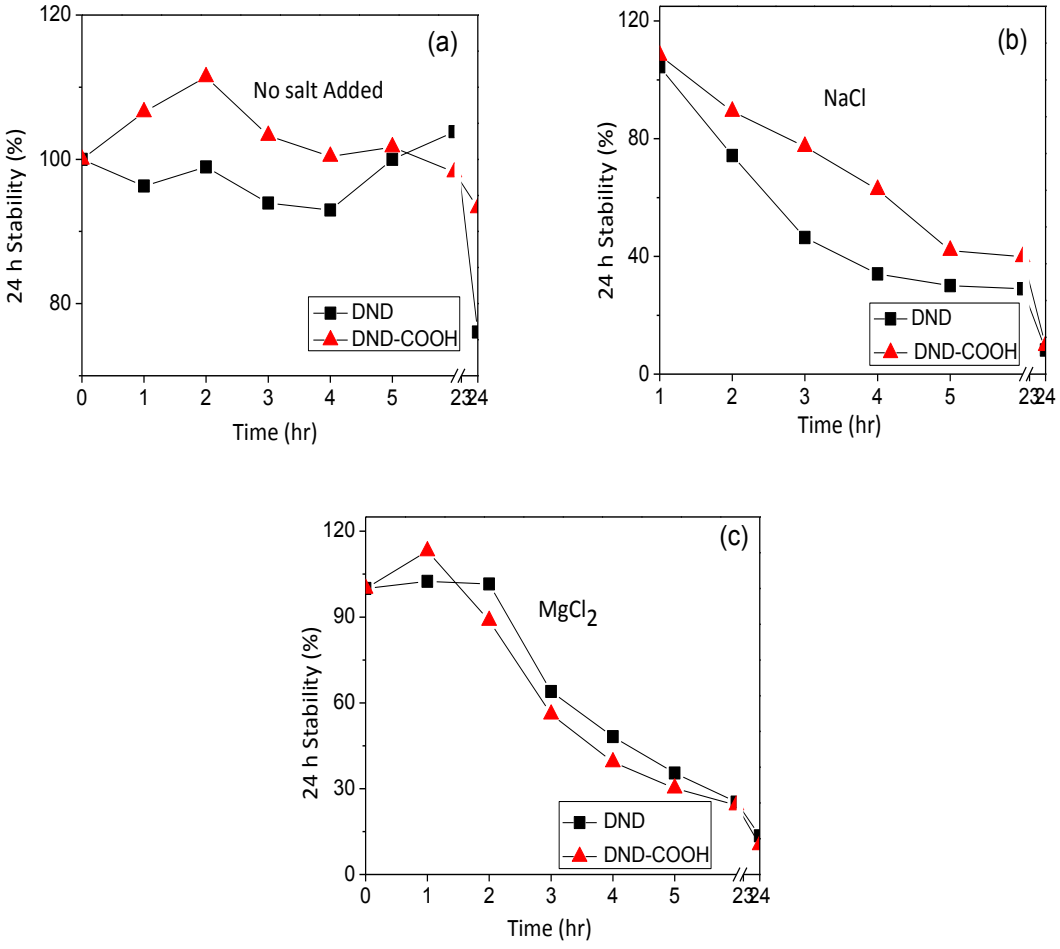

Figure 4.4 Stability as a function of time measured by fluorescence at 753.2 nm**.**

Figure 4.4 shows the time dependent stability of the DND dispersions. It was observed that both DND and DND-COOH dispersions in deionized water were stable over the 24 h measurement period. Significant aggregation and subsequent deposition of the nanoparticles was observed in the electrolytic environment within 3 to 5 hours. DND-COOH was more stable than DND in presence of NaCl, while in the presence of $MgCl_2$ their behaviors were similar.

4.4 Conclusions

The fundamental understanding of the colloidal behavior of DNDs is the key to predicting their fate and transport in aquatic environments. Results suggest that the colloidal behavior of DNDs will depend upon the presence of electrolytes. While the DND and DND-COOH were very different materials, the aggregation behavior based on particle size and zeta potential measurements showed similar behavior in the presence of electrolytes. Nevertheless, the results may not be generalized for all commercial nanodiamonds because there may be significant differences in physicochemical properties depending upon synthesis and pretreatment methods used in material preparations.

CHAPTER 5

EFFECT OF SOLVENTS ON STABILIZATION OF MICRO DRUG PARTICLES

5.1 Introduction

It is estimated that a high percentage of newly developed active pharmaceutical ingredients (API) have poor water solubility (Leuner and Dressman, 2000; Wong et al., 2006; Mehta et al., 2007) which leads to lower dissolution rate and poor bioavailability (Merisko-Liversidge et al., 2003; Zimmermann et al., 2007). The dissolution is often the rate- limiting step and various approaches, such as the reduction in particle size and compositing with hydrophilic carriers and/or surfactants have been used (Schmidt and Bodmeier, 1999) to address this issue. Therefore, particle size is an important issue in a drug formulation, (Choi et al., 2005) and its reduction is of great interest. Conventional methods for the synthesis of micron and submicron particles include milling and homogenization in order to reduce the particle size (Rabinow, 2004; Choi et al., 2005). Sometimes, controlling of size, morphology, surface properties and electrostatic charge is often difficult. Precipitation processes that form particles directly may provide more control of these parameters (Rasenack and Müller, 2002a; De Gioannis et al., 2004).

In recent years, bottom-up processes such as emulsification and antisolvent precipitation methods have emerged as methods for the synthesis of micro or sub micro size particles from the liquids (Zambaux et al., 1998; Kipp, 2004). Antisolvent precipitation of hydrophobic drugs involves contact of an aqueous phase with an organic solution containing the drug (Wang et al., 2004).

Meng and her group had usually used sonication assisted anti-solvent methods for the synthesis of submicron and micron size particles of insoluble drug moieties (Meng et al., 2009). In such process, micro/nano scale drug particles are formed by precipitation from an organic solution when the latter is micro mixed in an aqueous phase under ultrasonic agitation. The three basic steps involved in such a process is supersaturation, nucleation, and particle growth (Dirksen and Ring, 1991)**.** Supersaturation is the driving force for nucleation/growth and can be achieved either by increasing solute concentration or decreasing the solubility using methods such as solvent evaporation, dissolution of a metastable solid phase, cooling, alternate antisolvent and salting out (Jeon et al., 2000; Muhrer et al., 2006; Patrick Augustijns, 2007).

The key to this approach is the stabilization of the colloid. An unstable suspension could lead to large dose variations; and so, long-term stability is of utmost importance in pharmaceutical industry (Lucas et al., 2004). Hydrophilic polymers have been known to contribute to steric stability as well via a thickening action (Duro et al., 1998). Meng and her group have reported the use of combination of surfactants and celluloses as effective means of suspension stabilization (Meng et al., 2009). In the antisolvent method, supersaturation can be varied by using different solvents. Moreover, the physicochemical parameters of the suspension are also altered, which alters suspension stability. In short, the combination of the appropriate solvent along with arrested growth by polymers and surfactants is a powerful approach to control the formation of micron and submicron size particles in an aqueous phase (Yagi et al., 1996; Pongpeerapat et al., 2004). This chapter focuses on the effect of solvent on suspension stability.

5.2 Preparation of Micro Drug Particles

Antisolvent precipitation is a technique where a drug solution in a water miscible organic solvent is mixed with an aqueous solution containing a surfactant. Upon mixing, the supersaturated solution leads to nucleation and growth of drug particles. All precipitation experiments were carried out at room temperature. Griseofulvin which was a model drug was dissolved in three different solvents (.i.e. Acetone, DMSO, ethanol) to form a clear solution. The cellulose ethers and SDS were dissolved in Milli-Q water by stirring. The ratio of drug, cellulose ether and SDS was 3:1:1. The drug solution was added into the aqueous phase slowly during sonication. The final drug concentration in the suspension was 0.4 % w/w. The pH of the aqueous dispersions was approximately 7.

5.2.1 Particle Size Measurements

Particle size and size distribution measurements of the bulk suspension were performed using static and dynamic light scattering. Static Light scattering which gave an estimate of the particle size distribution of the stabilized suspension was carried out using Coulter Particle Size Analyzer LS 230. On the other hand, dynamic light scattering provided a selective picture of the relatively smaller particles that underwent significant Brownian motion. Dynamic light scattering was carried out using Beckman Coulter, N4 plus Submicron Particle Size Analyzer at 23^{o} fixed detector angle. The micro particles nucleation and growth in the suspension was successfully monitored by measuring the change of particle diameter as a function of time. Zeta potential measurements were determined using a Delsa Nano (Beckmann Coulter). Zeta potentials were determined from the electrophoretic mobilities of particles by using the Smoluchowski equation. All measurements were performed at 25 ^{o}C.

5.2.2 Characterization

Scanning electron microscope (SEM; LEO 1530VP) was used for studying particle size and morphology. The suspensions were placed onto an aluminum stub and dried at the room temperature. Then the samples were coated with carbon using a sputter coater (MED020 HR). In order to get the possible representation of the particles in the suspension, different regions of the suspensions were taken onto the stub and recorded with SEM. A Nicolet Almege XR Dispersive Raman with Olympus BX51 Confocal Microscope (Thermo Electron Corp.) using a laser at 532 nm was applied in the Raman imaging mode. The samples were placed onto the glass slide for the detection using 100X optical lens. X-ray diffraction (XRD) data was collected at beam line X7B line (λ = 0.3184 A˚) of the National Synchrotron Light Source (NSLS) at Brookhaven National Laboratory (BNL), Upton, NY. A MAR345 detector was used to record full X-ray patterns and the powder rings were integrated with the FIT2D code. The FIT2D parameters for the integration of the data were obtained with a standard LaB6 crystal compound.

5.2.3 Monitoring the Sedimentation Rate

Sedimentation was monitored as a function of time by measuring the weight percentage of the solid remaining in the suspension. This was accomplished as follows. Each suspension was divided equally into four subsamples and transferred to separate tubes and stored at 25 ^{o}C. The solid sediments were collected at 2, 4, 7 and 9 hour intervals, dried in the oven at 35 ^{o}C in a vacuum to remove the solvent and then the solid sediments were rinsed with Milli-Q water to remove the excess cellulose ethers and SDS before weighing.

5.3 Results and Discussion

The rate for homogeneous nucleation is expressed by the Gibbs, Volmer equation (Patrick Augustijns, 2007).

$$J = N_0 \nu \exp\left(\frac{-16\pi\vartheta^2\gamma_{12}^{\ 3}}{3(K_B T)^3\left(ln\left(\frac{c}{s}\right)\right)^2}\right) \quad (5.1)$$

Where J is the number of nuclei formed per unit time per unit volume, N_0 is the number of molecules in a unit volume, ν is the frequency of atomic or molecular transport at the nucleus- liquid interface, ϑ= molecular volume of the crystallizing solute, γ_{12} is the Interfacial energy per unit area between solvent and cluster, k_B is the Boltzmann Constant, T is the Temperature and c is the concentration, s is the solubility, while c/s is the supersaturation. The first three have strong dependence on the choice of the organic solvent. The equilibrium solubility of GF in water is known to be 0.009 mg/ml. The solubility of GF in 100:70 solvent-water mixture was measured experimentally (Table 5.1). It was found that the solubility in DMSO-water was significantly lower than in acetone/ethanol water mixture. DMSO had the highest density, viscosity, dielectric constant, boiling point and pKa (Table 5.2) for the same final GF concentration. DMSO represented the highest degree of super saturation followed by acetone and Ethanol (Table 5.3).

Table 5.1 Experimented Values for Different GF/ Solvent Systems

Parameters GF with different solvents	GF/ Acetone	GF/ DMSO	GF/Ethanol
Viscosity (cp)	1.05	1.11	0.98
Density(g/ml)	0.99	1.01	0.99
Zeta potential(mv)	-15.16	-1.34	9.43
Solubility(%wt/v)	4.96	12.05	0.81

Table 5.2 Physiochemical Properties of Solvents

Physiochemical properties	Acetone	DMSO	Ethanol
Density(gm/ml)	0.78	1.09	0.78
Viscosity (cp)	0.32	2.00	1.20
Dielectric constant	20.7	47.2	24.3
B.P(^{0} C)	56	189	78
Pka	19.3	28	16

5.3.1 Particle Size Distribution

Dynamic light scattering or photon correlation spectroscopy (PCS) was used to selectively monitor the growth of the smaller particles. PCS works by measuring the velocity at which the particles move under Brownian motion (Bilati et al., 2005)**.** Figure 5.1 shows the comparison of particle size as formed via antisolvent precipitation using the three solvents. It is interesting to see that all the particle growth in all three cases were quite different. Over a period of 50 h, the PCS measurements showed a uniform particle size distribution when ethanol was used as the solvent. In case of DMSO, the particles were seen to grow slowly over a period of time. This may be attributed to the higher

degree of supersaturation where one may expect larger nucleation rate, while higher viscosity, density and dielectric constants may have led to slower rate of agglomeration. In case of ethanol and acetone, the particles grew rapidly (within an hour) to 1500 nm. These particles stabilized in ethanol, but the average particle size decreased in case of acetone. This was attributed to Ostwald ripening (Van Eerdenbrugh et al., 2008a)

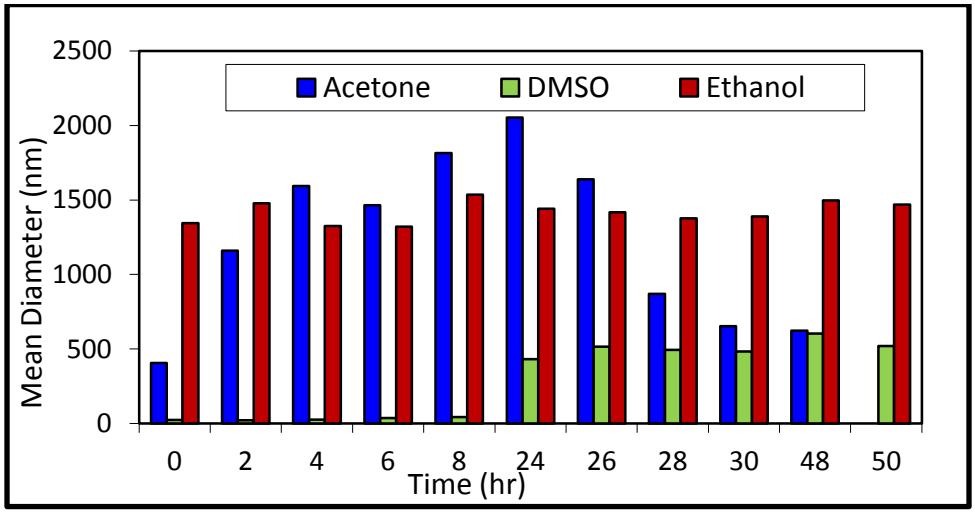

Figure 5.1 Dynamic light scattering measurements of stabilized suspension as a function of time in solvent/water mixture.

The overall particle size distribution (PSD) was monitored using laser diffractometry. Laser diffraction based particle size analysis is based on particles passing through a laser beam which scatter light at an angle that is directly related to their size. Typical PSD in stabilized suspension for three solvent systems is shown in Figure 5.2. The largest particles eventually settled down. Ethanol produced the largest average PSD, and DMSO was the smallest. The higher degree of supersaturation in case of DMSO probably led to higher nucleation rate, and coupled with low agglomeration (Figure 5.1) generated the smallest PSD.

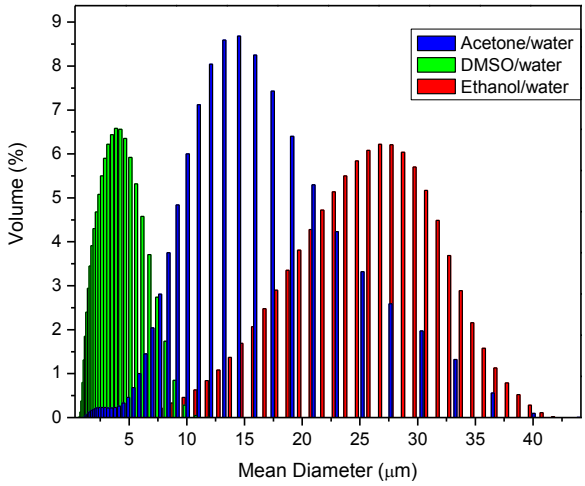

Figure 5.2 Particle size distribution of a model drug for three solvent/water systems.

5.3.2 Long Term Stability as a Function of Time

Long term stability of a suspension was studied as a function of time. The stability was studied for up to 50 h. The mean diameter or particle size was measured every 2 h without sonication. When DMSO was used as a solvent, it produced smaller and stable particles whose size did not change significantly for up to 50 h. On the other hand Acetone produced suspensions that were not as stable. Particle growth depends on the metastable concentration region that exists between solubility and spontaneous nucleation (Patrick Augustijns, 2007). For a given solute, this varies from solvent to solvent. The particle growth is stable within the metastable region and one can achieve controllable particle size by using the appropriate solvent systems. In this case (Figure 5.3), compared to ethanol- water and acetone-water systems, the DMSO-water system appeared to be in the metastable region and produced the smallest particle size and exhibited slower particle growth. Zeta potential measurements were used to study the stability of the drug suspension. The zeta potential values were measured 24 h after the preparation of the

drug suspensions (Table 5.1). These numbers imply that the suspension was not highly stable from an electrostatic consideration, but rather prone to agglomeration. In case of acetone, the zeta potentials were more negative, this was consistent with previous observations (Meng et al., 2009).

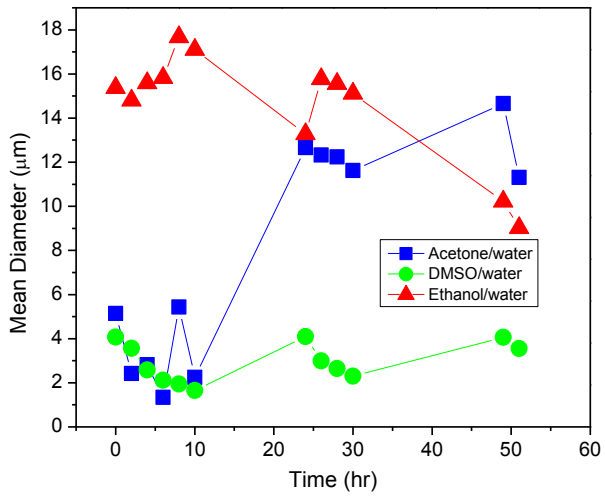

Figure 5.3 Long term stability for three drug-solvent systems as a function of time.

5.3.3 Sedimentation Rate

Sedimentation rate is a key factor in determining long term stability (Van Eerdenbrugh et al., 2008b). Typically; the particles grow or aggregate to a large size, which increases the overall setting rate. Rate of settling can be described using Stokes equation (Mersmann, 1999).

$$\frac{dx}{dt} = \frac{d^2(\rho_j - \rho_e)g}{18\eta} \tag{5.2}$$

Where dx/dt is the rate of settling, d is the diameter of the dispersed particle, ρ_i is the density of the particles and the ρ_e is the density of the medium, g is the gravitational constant and η is the viscosity of the medium. Here the rate of settling is proportional to the square of the diameter, density difference between the particle and the medium, and inversely proportional to viscosity of the medium. Solvent affects both viscosity and density of the medium and are important parameters. The density and viscosity of the three systems is presented in Table 5.1. DMSO had the highest density and viscosity.

The solid particles were uniformly distributed in the suspension after the antisolvent precipitation. The amount of the solid particles in the suspension decreased with time as they began to settle. These are presented in Figure 5.4.

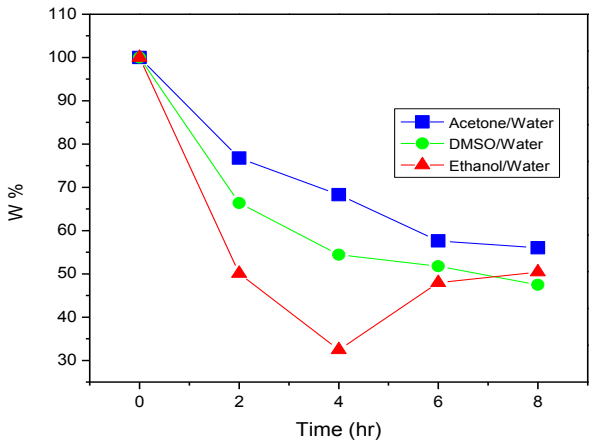

Figure 5.4 Weight percentages of stabilized drug-solvent systems as a function of time.

The results appear to be consistent with the Stokes equation that the smaller diameter particles have lower settling rate (Elizalde et al., 2000). However, the rate of settling varied depending upon the solvent used. At the end of 8 h, nearly 50% of the particles were in suspension for all the solvents. Ethanol showed a rather unusual behavior, where initially the particles settled down but eventually they were resuspened

back. The settling rate was the highest for ethanol followed by DMSO and acetone. According to the Stokes equation, the density differential and viscosity play important roles, based on this one would expect DMSO to have the lowest settling rate, but that was clearly the case.

Figure 5.5 shows the plot of experimental settling rate vs. theoretical settling rate which was calculated using stokes equation. The data points did not show any trend, implying that suspension stability depend on other factors that could include dielectric constant and hydrophobicity (Mine et al., 2005). Also, the Stokes law is strictly applicable for dilute suspensions with uniform; spherical particles having less inter particle collisions and without any affinity with the dispersion medium (Banker, 2002). Some of these assumptions were not valid in this case.

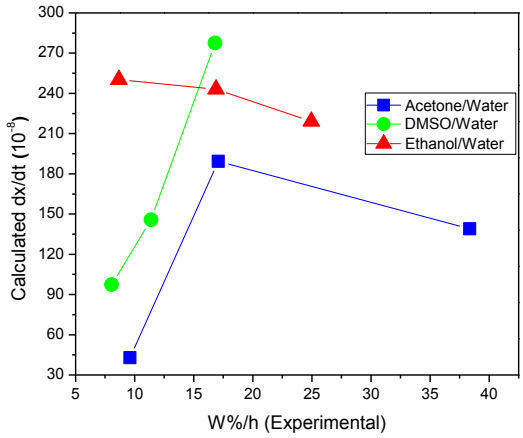

Figure 5.5 Experimental vs. theoretical value of settling rate (using Stokes Equation).

Figure 5.6 shows the settling rate as a function of time for all systems. It was evident that the settling rate increased rapidly within the first two hours and then dropped to 1-2 %. The rate of settling was the highest in ethanol.

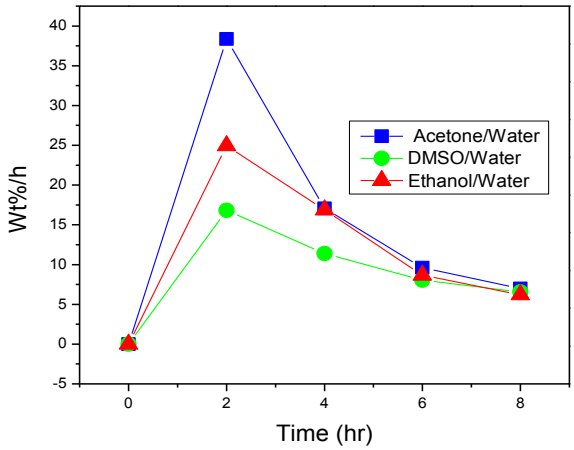

Figure 5.6 Rate of settling as a function of time for three drug-solvent systems.

Table 5.3 Parameters for GF with Different Solvents

Suspension In Solvent	Mean diameter (μm)		Percentage of particles in suspension (%)		Sedimentation rate (w %/h)	
	0 hour	4 hour	4 hour	8 hour	2 hour	6 hour
GF/Acetone	5.13	2.82	68.30	56.00	11.60	3.60
GF/DMSO	4.07	2.83	54.42	47.76	16.81	8.03
GF/Ethanol	15.37	14.28	32.46	50.40	24.95	8.67

5.3.4 Particle Morphology

Figure 5.7 shows the comparison of SEM images of drug particles produced from the three solvents. It was found that the crystal shape was identical for all the three systems. There were no apparent agglomerations in any of the systems. Figure 5.8 shows the Raman spectra of the particles produced from the three solvents showed similar signature, indicating that both the chemical nature of the stabilized particles and the

polymorphs were identical. The Raman spectra showed the C=O stretching of benzofuran ring of GF in the region 1550-1800 cm^{-1} and C-H stretching in the region of 2800-3200 cm^{-1} were observed in both pure GF and it stabilized analog (Bolton and Prasad, 1981).

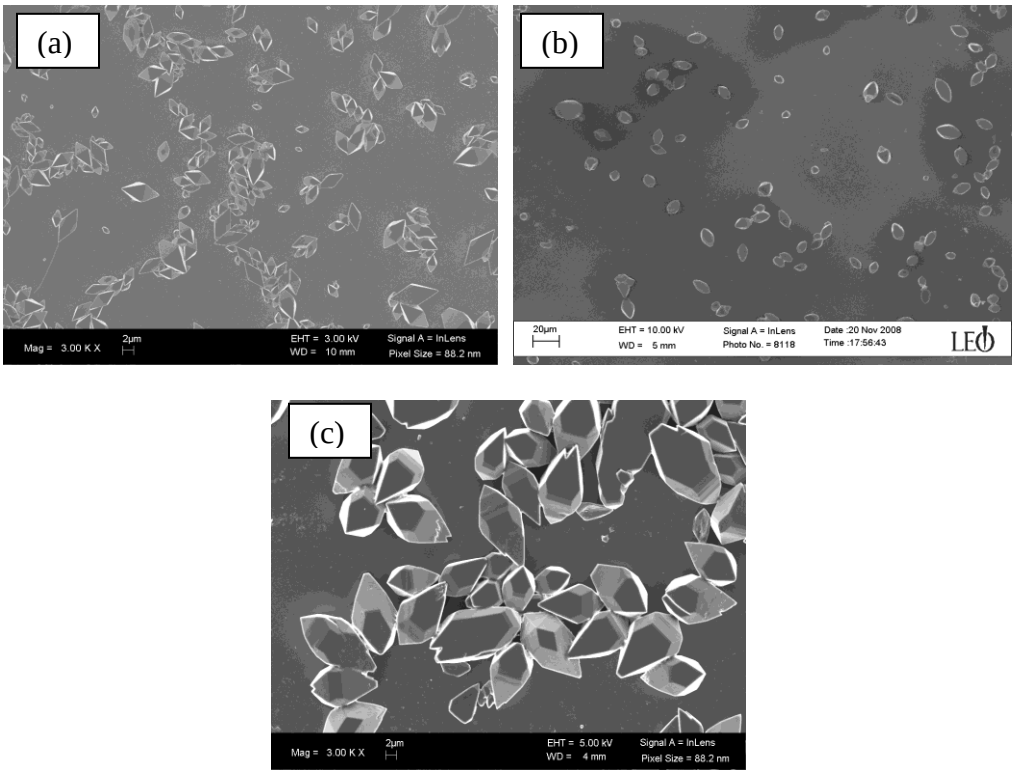

Figure 5.7 SEM image of Drug Particles in (a) Acetone (b) DMSO and (c) Ethanol.

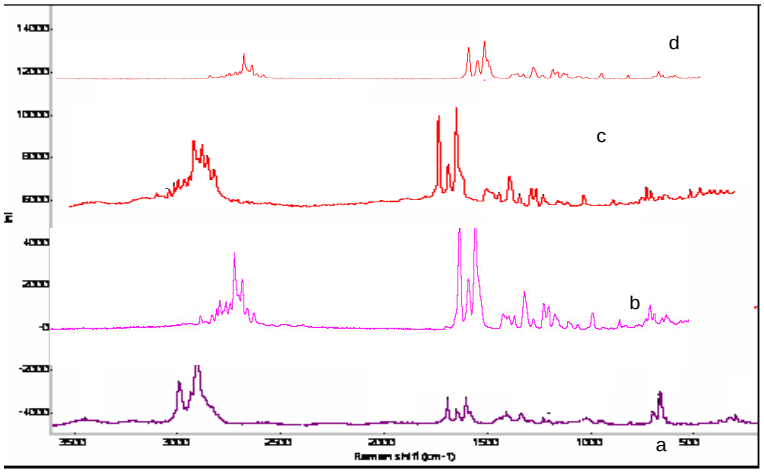

Figure 5.8 Raman spectra of (a) GF/DMSO (b) GF/Ethanol (c) GF/Acetone (d) Pure GF.

Figure 5.9 shows the XRD data for three solvent systems. The graph shows almost the same trend for all three systems. That means crystal morphology or surface structure does not change for any solvent systems. However, there is a slight peak shifting observed between 2 theta values 5 to 6, and it was observed that solvent may play minor role for this shift. It is clear from the Raman scattering and XRD data that the crystals contained the respective drugs and there is no interaction between cellulose ether and SDS.

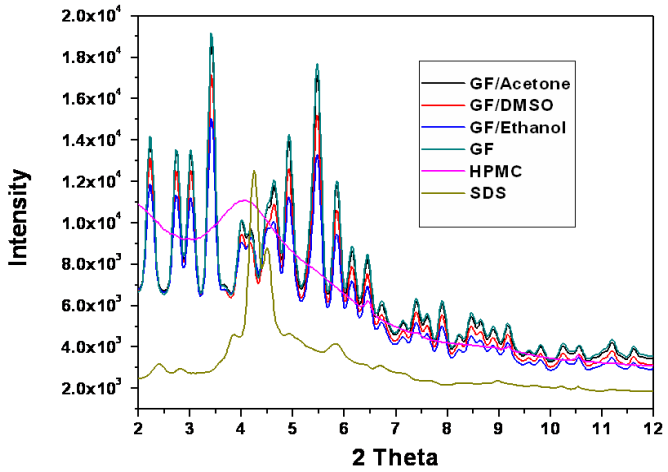

Figure 5.9 XRD data of drug particles prepared in different solvents.

5.4 Conclusions

Three solvents were used for antisolvent precipitation of hydrophobic drug molecules, which was quite effective under ultrasonic agitation. At the end of 9 h, average diameters of particles in suspension were smallest when DMSO was used the solvent, while ethanol produced the largest particles. Long term stability was higher in DMSO compare to other two systems. Raman Spectroscopy as well as XRD data confirmed the presence of the drug molecule in these crystals.

REFERENCES

Addo Ntim, S.; Sae-Khow, O.; Witzmann, F. A.; Mitra, S. Effects of Polymer Wrapping and Covalent Functionalization on the Stability of MWCNT in Aqueous Dispersions. *J. Colloid Interface Sci*. **2011**, 355, 383-388.

Aleksenskiĭ, A. E.; Baĭdakova, M. V.; Vul, A. Y.; Siklitskiĭ, V. I. The Structure of Diamond Nanoclusters. *Phys. Solid. State*. **1999**, 41, 668-671.

Ali-Boucetta, H.; Nunes, A.; Sainz, R.; Herrero, M. A.; Tian, B.; Prato, M.; Bianco, A. Kostarelos, K. Asbestos-Like Pathogenicity of Long Carbon Nanotubes Alleviated by Chemical Functionalization. Angew. Chem. Int. Ed. **2013**, 52, 2274-2278.

Ausman, K. D.; Piner, R.;Lourie, O.; Ruoff, R. S.; Korobov, M. Organic Solvent Dispersions of Single-Walled Carbon Nanotubes: Toward Solutions of Pristine Nanotubes. *J. Phys. Chem. B.* **2000**, 104, 8911-8915.

Baidakova, M.; Vul, A. New Prospects and Frontiers of Nanodiamond Clusters. *J. Phys. D: Appl. Phys*. **2007**, 40, 6300-6311.

Banhart, F.; Ajayan, P. M. Carbon Onions as Nanoscopic Pressure Cells for Diamond Formation. *Nature*. **1996**, 382, 433-435.

Banker, G. S.; Rhodes.C.T. 2002. Modern Pharmaceutics, Taylor & Francis, New York, New York, USA.

Basiuk, E. V.; Basiuk, V. A.; Meza-Laguna, V.; Contreras-Torres, F. F.; Martínez, M.; Rojas-Aguilar, A.; Salerno, M.; Zavala, G.; Falqui, A. Brescia, R. Solvent-Free Covalent Functionalization of Multi-Walled Carbon Nanotubes and Nanodiamond with Diamines: Looking for Cross-Linking Effects. *Appl. Surf. Sci*. **2012**, 259, 465-476.

Bilati, U.; Allémann, E.; Doelker, E. Development of a Nanoprecipitation Method Intended for the Entrapment of Hydrophilic Drugs into Nanoparticles. *Eur. J. Pharm. Sci*.. **2005**, 24, 67-75.

Bogdal, D.; Penczek, P.; Pielichowski, J.; Prociak, A. Microwave Assisted Synthesis, Crosslinking, and Processing of Polymeric Materials. *Adv. Poly. Sci*. **2003**, 163, 193-263.

Bolton, B. A.; Prasad, P. N. Laser Raman Investigation of Pharmaceutical Solids: Griseofulvin and Its Solvates. *J. Pharm. Sci*. **1981**, 70, 789-793.

Boudou, J. P.; Curmi, P. A.; Jelezko, F.; Wrachtrup, J.; Aubert, P.; Sennour, M.; Balasubramanian, G.; Reuter, R.; Thorel, A. Gaffet, E. High Yield Fabrication of Fluorescent Nanodiamonds. *Nanotechnology*. **2009**, 20, 1-11.

Burleson, T.; Yusuf, N.; Stanishevsky, A. Surface Modification of Nanodiamonds for Biomedical Application and Analysis by Infrared Spectroscopy. *J. Achiev. Mater. Manuf. Eng*. **2009**, 37, 258-263.

Buzea, C.; Pacheco, I.; Robbie, K. Nanomaterials and Nanoparticles: Sources and Toxicity. *Biointerphases*. **2007**, 2, MR17-MR71.

Caddick, S. Microwave Assisted Organic Reactions. *Tetrahedron*. **1995**, 51, 10403-10432.

Chang, C.-M.; Liu, Y.-L. Functionalization of Multi-Walled Carbon Nanotubes with Furan and Maleimide Compounds through Diels–Alder Cycloaddition. *Carbon*. **2009**, 47, 3041-3049.

Chen, K. L.; Elimelech, M. Influence of Humic Acid on the Aggregation Kinetics of Fullerene (C60) Nanoparticles in Monovalent and Divalent Electrolyte Solutions. *J. Colloid Interface Sci*. **2007**, 309, 126-134.

Chen, K. L.; Elimelech, M. Relating Colloidal Stability of Fullerene (C60) Nanoparticles to Nanoparticle Charge and Electrokinetic Properties. *Environ. Sci. Technol.* **2009**, 43, 7270-7276.

Chen, K. L.; Mylon, S. E.; Elimelech, M. Aggregation Kinetics of Alginate-Coated Hematite Nanoparticles in Monovalent and Divalent Electrolytes. *Environ. Sci. Technol.* **2006**, 40, 1516-1523.

Chen, Q.; Saltiel, C.; Manickavasagam, S.; Schadler, L. S.; Siegel, R. W.; Yang, H. Aggregation Behavior of Single-Walled Carbon Nanotubes in Dilute Aqueous Suspension. *J. Colloid Interface Sci*. **2004**, 280, 91-97.

Chen, R. J.; Zhang, Y.; Wang, D.; Dai, H. Noncovalent Sidewall Functionalization of Single-Walled Carbon Nanotubes for Protein Immobilization. *J. Am. Chem. Soc.* **2001**, 123, 3838-3839.

Chen, Y.; Mitra, S. Fast Microwave- Assisted Purification, Functionalization and Dispersion of Multi-Walled Carbon Nanotubes. *J. Nanosci. Nanotechnol.* **2008**, 8, 5770-5775.

Chiang, I. W.; Brinson, B. E.; Smalley, R. E.; Margrave, J. L.; Hauge, R. H. Purification and Characterization of Single-Wall Carbon Nanotubes. *J. Phys. Chem. B*. **2001**, 105, 1157-1161.

Choi, J. Y.; Yoo, J. Y.; Kwak, H. S.; Nam, B. U.; Lee, J. Role of Polymeric Stabilizers for Drug Nanocrystal Dispersions. *Curr.Appl. Phys*. **2005**, 5, 472-474.

Choi, W. B.; Cuomo, J. J.; Zhirnov, V. V.; Myers, A. F.; Hren, J. J. Field Emission from Silicon and Molybdenum Tips Coated with Diamond Powder by Dielectrophoresis. *Appl. Phys. Lett*. **1996**, 68, 720-722.

Chong, Y. M.; Ma, K. L.; Leung, K. M.; Chan, C. Y.; Ye, Q.; Bello, I.; Zhang, W.; Lee, S. T. Synthesis and Mechanical Properties of Cubic Boron Nitride /Nanodiamond Composite Films. *Chem. Vap. Deposition*. **2006**, 12, 33-38.

Chu, H. Y.; Hsu, W. C.; Lin, J. F. Scuffing Mechanism During Oil-Lubricated Block-on-Ring Test with Diamond Nanoparticles as Oil Additive. *Wear*. **2010**, 268, 1423-1433.

Danhier, F.; Lecouturier, N.; Vroman, B.; Jérôme, C.; Marchand-Brynaert, J.; Feron, O. Préat, V. Paclitaxel-Loaded Pegylated Plga-Based Nanoparticles: In Vitro and in Vivo Evaluation. *J. Controlled Release*. **2009**, 133, 11-17.

Daniel, S.; Rao, T. P.; Rao, K. S.; Rani, S. U.; Naidu, G. R. K.; Lee, H.-Y.; Kawai, T. A Review of DNA Functionalized/Grafted Carbon Nanotubes and Their Characterization. *Sens. Actuators, B.* **2007**, 122, 672-682.

Das, S.; Roy, P.; Mondal, S.; Bera, T.; Mukherjee, A. One Pot Synthesis of Gold Nanoparticles and Application in Chemotherapy of Wild and Resistant Type Visceral Leishmaniasis. *Colloids Surf., B.* **2013**, 107, 27-34.

Daulton, T. L.; Kirk, M. A.; Lewis, R. S.; Rehn, L. E. Production of Nanodiamonds by High-Energy Ion Irradiation of Graphite at Room Temperature. *Nucl. Instrum. Methods Phys. Res., Sect. B.* **2001**, 175–177, 12-20.

David, R. M. Measuring Engineered Nanomaterials in the Environment: A Consortium View of How to Address the Problem. *Environ. Eng. Sci.*. **2013**, 30, 97-100.

De Gioannis, B.; Jestin, P.; Subra, P. Morphology and Growth Control of Griseofulvin Recrystallized by Compressed Carbon Dioxide as Antisolvent. *J. Cryst. Growth*. **2004**, 262, 519-526.

Derjaguin, B.; Landau, L. Theory of the Stability of Strongly Charged Lyophobic Sols and of the Adhesion of Strongly Charged Particles in Solutions of Electrolytes. *Prog. Surf. Sci.*. **1993**, 43, 30-59.

Desai, C.; Mitra, S. Microwave Induced Carboxylation of Nanodiamonds. *Diamond Relat. Mater.* **2013**, 34, 65-69.

Desai, C.; Addo Ntim, S.; Mitra, S. Antisolvent Precipitation of Hydrophobic Functionalized Multiwall Carbon Nanotubes in an Aqueous Environment. *J. Colloid Interface Sci*. **2012**, 368, 115-120.

Desai, C.; Meng, X.; Yang, D.; Wang, X.; Akkunuru, V.; Mitra, S. Effect of Solvents on Stabilization of Micro Drug Particles. *J. Cryst. Growth*. **2010**, 314, 353-358.

Dirksen, J. A.; Ring, T. A. Fundamentals of Crystallization: Kinetic Effects on Particle Size Distributions and Morphology. *Chem. Eng. Sci.*. **1991**, 46, 2389-2427.

Dolmatov, V. Y.; Veretennikova, M.; Marchukov, V.; Sushchev, V. Currently Available Methods of Industrial Nanodiamond Synthesis. *Phys. Solid State*. **2004**, 46, 611-615.

Dolmatov, V. Y. Detonation-Synthesis Ultradispersed Diamonds: Properties and Applications. *Russ. Chem. Rev*. **2001**, 70, 607-626.

Dolmatov, V. Y. Detonation-Synthesis Nanodiamonds: Synthesis, Structure, Properties and Applications. *Russ. Chem. Rev*. **2007**, 76, 339-360.

Dong, Y.; Ng, W. K.; Shen, S.; Kim, S.; Tan, R. B. H. Controlled Antisolvent Precipitation of Spironolactone Nanoparticles by Impingement Mixing. *Int. J. Pharm*. **2011**, 410, 175-179.

Du, Z.; Zhao, D.; Jing, L.; Cui, G.; Jin, M.; Li, Y.; Liu, X.; Liu, Y.; Du, H.; Guo, C.; Zhou, X.; Sun, Z. Cardiovascular Toxicity of Different Sizes Amorphous Silica

Nanoparticles in Rats after Intratracheal Instillation. Cardiovasc. *Toxicol.*. **2013**, 1-14.

Duro, R.; Alvarez, C.; Martínez-Pacheco, R.; Gómez-Amoza, J. L.; Concheiro, A.; Souto, C. The Adsorption of Cellulose Ethers in Aqueous Suspensions of Pyrantel Pamoate: Effects on Zeta Potential and Stability. *Eur. J. Pharm. Sci. Biopharm*. **1998**, 45, 181-188.

Ebbesen, T. W. Carbon Nanotubes. Phys. Today. **1996**, 49, 26-32.

Elimelech, M.; Gregory, J.; Jia, X.; Williams, R. 1998. Particle Deposition and Aggregation: Measurement, Modelling and Simulation, Oxford United Kingdom, Butterworth-Heinemann.

Elizalde, O.; Leal, G. P.; Leiza, J. R. Particle Size Distribution Measurements of Polymeric Dispersions: A Comparative Study. *Part. Part. Syst. Char*. **2000**, 17, 236-243.

Esumi, K.; Ishigami, M.; Nakajima, A.; Sawada, K.; Honda, H. Chemical Treatment of Carbon Nanotubes. *Carbon*. **1996**, 34, 279-281.

Fakruddin, M.; Hossain, Z.; Afroz, H. Prospects and Applications of Nanobiotechnology: A Medical Perspective. *J. Nanobiotechnology*. **2012**, 10.1-8.

Fan, K.; Gong, C.; Peng, T.; Chen, J.; Xia, J. A. Novel Preparation of Small Tio2 Nanoparticle and Its Application to Dye-Sensitized Solar Cells with Binder-Free Paste at Low Temperature. *Nanoscale*. **2011**, 3, 3900-3906.

Frenklach, M.; Howard, W.; Huang, D.; Yuan, J.; Spear, K. E.; Koba, R. Induced Nucleation of Diamond Powder. *Appl. Phys. Lett*. **1991**, 59, 546-548.

Gaiser, B. K.; Hirn, S.; Kermanizadeh, A.; Kanase, N.; Fytianos, K.; Wenk, A.; Haberl, N.; Brunelli, A.; Kreyling, W. G.; Stone, V. Effects of Silver Nanoparticles on the Liver and Hepatocytes in Vitro. *Toxicol. Sci*. **2013**, 131, 537-547.

Galimov, É. M.; Kudin, A. M.; Skorobogatskiĭ, V. N.; Plotnichenko, V. G.; Bondarev, O. L.; Zarubin, B. G.; Strazdovskiĭ, V. V.; Aronin, A. S.; Fisenko, A. V.; Bykov, I. V.; Barinov, A. Y. Experimental Corroboration of the Synthesis of Diamond in the Cavitation Process. *Dokl. Phys*. **2004**, 49, 150-153.

Giordano, A. N.; Chaturvedi, H.; Poler, J. C. Critical Coagulation Concentrations for Carbon Nanojtubes in Nonaqueous Solvent. *J. Phys. Chem. C*. **2007**, 111, 11583-11589.

Gogotsi, Y. G.; Nickel, K. G.; Bahloul-Hourlier, D.; Merle-Mejean, T.; Khomenko, G. E. Skjerlie, K. P. Structure of Carbon Produced by Hydrothermal Treatment of β-Sic Powder. *J. Mater. Chem.* **1996**, 6, 595-604.

Gour, S. 2010. Manufacturing Nano-Sized Powders Using Salt and Sugar Assisted Milling, Drexel Univ. PA.

Greiner, N. R.; Phillips, D. S.; Johnson, J. D.; Volk, F. Diamonds in Detonation Soot. *Nature*. **1988**, 333, 440-442.

Grichko, V.; Tyler, T.; Grishko, V. I.; Shenderova, O. Nanodiamond Particles Forming Photonic Structures. *Nanotechnology*. **2008**, 19, 1-5.

Gruen, D. M.; Shenderova, O. A. Vul', A. Y. 2005. Synthesis, Properties and Applications of Ultrananocrystalline Diamond, Springer, New York, New York, USA.

Grujicic, M.; Sun, Y. P.; Koudela, K. L. The Effect of Covalent Functionalization of Carbon Nanotube Reinforcements on the Atomic-Level Mechanical Properties of Poly-Vinyl-Ester-Epoxy. *Appl. Surf. Sci*. **2007**, 253, 3009-3021.

He, D.; Shao, L.; Gong, W.; Xie, E.; Xu, K.; Chen, G. Electron Transport and Electron Field Emission of Nanodiamond Synthesized by Explosive Detonation. *Diamond Relat. Mater*. **2000**, 9, 1600-1603.

Hens, S. C.; Cunningham, G.; Tyler, T.; Moseenkov, S.; Kuznetsov, V.; Shenderova, O. Nanodiamond Bioconjugate Probes and Their Collection by Electrophoresis. *Diamond Relat. Mater*. **2008**, 17, 1858-1866.

Hirsch, A. Vostrowsky, O. Functionalization of Carbon Nanotubes. Functional Molecular Nanostructures. In: Schlüter, A. D.(ed.). Germany:Springer Berlin/Heidelberg.

Hong, S.; Elimelech, M. Chemical and Physical Aspects of Natural Organic Matter (NOM) Fouling of Nanofiltration Membranes. *J. Membr. Sci*. **1997**, 132, 159-181.

Hu, C.; Chen, Z.; Shen, A.; Shen, X.; Li, J.; Hu, S. Water-Soluble Single-Walled Carbon Nanotubes Via Noncovalent Functionalization by a Rigid, Planar and Conjugated Diazo Dye. *Carbon*. **2006**, 44, 428-434.

Hu, C.; Liao, H.; Li, F.; Xiang, J.; Li, W.; Duo, S.; Li, M. Noncovalent Functionalization of Multi-Walled Carbon Nanotubes with Siloxane Polyether Copolymer. *Mater. Lett*. **2008**, 62, 2585-2588.

Huang, L. C. L.; Chang, H. C. Adsorption and Immobilization of Cytochrome C on Nanodiamonds. *Langmuir*. **2004**, 20, 5879-5884.

Huang, W.; Taylor, S.; Fu, K.; Lin, Y.; Zhang, D.; Hanks, T. W.; Rao, A. M.; Sun, Y.-P. Attaching Proteins to Carbon Nanotubes Via Diimide-Activated Amidation. *Nano Lett*. **2002**, 2, 311-314.

Hussain, M.; Ceccarelli, R.; Marchisio, D. L.; Fino, D.; Russo, N.; Geobaldo, F. Synthesis, Characterization, and Photocatalytic Application of Novel TiO_2 Nanoparticles. *Chem. Eng. J*. **2010**, 157, 45-51.

Islam, M. F.; Rojas, E.; Bergey, D. M.; Johnson, A. T.; Yodh, A. G. High Weight Fraction Surfactant Solubilization of Single-Wall Carbon Nanotubes in Water. *Nano Lett*. **2003**, 3, 269-273.

Jee, A.-Y.; Lee, M. Surface Functionalization and Physicochemical Characterization of Diamond Nanoparticles. *Curr. Appl. Phys*. **2009**, 9, e144-e147.

Jeon, H. J.; Jeong, Y. I.; Jang, M. K.; Park, Y. H.; Nah, J. W. Effect of Solvent on the Preparation of Surfactant-Free Poly(DL-Lactide-Co-Glycolide) Nanoparticles and Norfloxacin Release Characteristics. *Int. J. Pharm*. **2000**, 207, 99-108.

Jeyaraj, M.; Sathishkumar, G.; Sivanandhan, G.; MubarakAli, D.; Rajesh, M.; Arun, R.; Kapildev, G.; Manickavasagam, M.; Thajuddin, N.; Premkumar, K.; Ganapathi, A. Biogenic Silver Nanoparticles for Cancer Treatment: An Experimental Report. *Colloids Surf., B*. **2013**, 106, 86-92.

Jiang, L.; Gao, L.; Sun, J. Production of Aqueous Colloidal Dispersions of Carbon Nanotubes. *J. Colloid Interface Sci*. **2003**, 260, 89-94.

Jung, D.-H.; Koan Ko, Y.; Jung, H.-T. Aggregation Behavior of Chemically Attached Poly(Ethylene Glycol) to Single-Walled Carbon Nanotubes (SWCNTs) Ropes. *Mater. Sci. Eng., C.* **2004**, 24, 117-121.

Kakran, M.; Shegokar, R.; Sahoo, N. G.; Al Shaal, L.; Li, L.; Müller, R. H. Fabrication of Quercetin Nanocrystals: Comparison of Different Methods. *Eur. J. Pharm. Biopharm.* **2012**, 80, 113-121.

Kang, M.; Myung, S. J.; Jin, H. J. Nylon 610 and Carbon Nanotube Composite by in Situ Interfacial Polymerization. *Polymer*. **2006**, 47, 3961-3966.

Kayser, O.; Lemke, A.; Hernández-Trejo, N. The Impact of Nanobiotechnology on the Development of New Drug Delivery Systems. *Curr. Pharm. Biotechnol.* **2005**, 6, 3-5.

Kharisov, B. I.; Kharissova, O. V.; Chávez-Guerrero, L. Synthesis Techniques, Properties, and Applications of Nanodiamonds. *Synth. React. Inorg., Met.-Org., Nano-Met. Chem. Res.* **2010**, 40, 84-101.

Kharisov, B. I.; Kharissova, O. V.; Gutierrez, H. L.; Méndez, U. O. Recent Advances on the Soluble Carbon Nanotubes. *Ind. Eng. Chem.* **2009**, 48, 572-590.

Kipp, J. E. The Role of Solid Nanoparticle Technology in the Parenteral Delivery of Poorly Water-Soluble Drugs. *Int. J. Pharm.* **2004**, 284, 109-122.

Kostarelos, K.; Lacerda, L.; Partidos, C. D.; Prato, M.; Bianco, A. Carbon Nanotube-Mediated Delivery of Peptides and Genes to Cells: Translating Nanobiotechnology to Therapeutics. *J. Drug. Deliv. Sci. Tec*. **2005**, 15, 41-47.

Kruger, A.; Liang, Y.; Jarre, G.; Stegk, J. Surface Functionalisation of Detonation Diamond Suitable for Biological Applications. *J. Mater. Chem*. **2006**, 16, 2322-2328.

Krüger, A.; Kataoka, F.; Ozawa, M.; Fujino, T.; Suzuki, Y.; Aleksenskii, A. E.; Vul', A. Y.; Ōsawa, E. Unusually Tight Aggregation in Detonation Nanodiamond: Identification and Disintegration. *Carbon*. **2005**, 43, 1722-1730.

Kulakova, I. Surface Chemistry of Nanodiamonds. *Phys. Solid. State*. **2004**, 46, 636-643.

Kuzmany, H.; Kukovecz, A.; Simon, F.; Holzweber, M.; Kramberger, C.; Pichler, T. Functionalization of Carbon Nanotubes. *Synth. Met*. **2004**, 141, 113-122.

Lee, J.; Kim, M.; Hong, C. K.; Shim, S. E. Measurement of the Dispersion Stability of Pristine and Surface-Modified Multiwalled Carbon Nanotubes in Various Nonpolar and Polar Solvents. *Meas. Sci. Technol.* **2007**, 18, 3707-3712.

Leuner, C.; Dressman, J. Improving Drug Solubility for Oral Delivery Using Solid Dispersions. *Eur. J. Pharm. Biopharm*. **2000**, 50, 47-60.

Li, L.; Davidson, J. L.; Lukehart, C. M. Surface Functionalization of Nanodiamond Particles Via Atom Transfer Radical Polymerization. *Carbon*. **2006**, 44, 2308-2315.

Lin, Y.; Zhou, B.; Shiral Fernando, K. A.; Liu, P.; Allard, L. F.; Sun, Y.-P. Polymeric Carbon Nanocomposites from Carbon Nanotubes Functionalized with Matrix Polymer. *Macromolecules*. **2003**, 36, 7199-7204.

Lisunova, M. O.; Lebovka, N. I.; Melezhyk, O. V.; Boiko, Y. P. Stability of the Aqueous Suspensions of Nanotubes in the Presence of Nonionic Surfactant. *J. Colloid Interface Sci*. **2006**, 299, 740-746.

Loktev, V. F.; Makal'skii, V. I.; Stoyanova, I. V.; Kalinkin, A. V.; Likholobov, V. A.; Mit'kin, V. N. Surface Modification of Ultradispersed Diamonds. *Carbon*. **1991**, 29, 817-819.

Lucas, T. I.; Bishara, R. H.; Seevers, R. H. A Stability Program for the Distribution of Drug Products. *Pharm. Technol*. **2004**, 28, 68-73.

M. F. Islam, E. R., D. M. Bergey, A. T. Johnson,A. G. Yodh. High Weight Fraction Surfactant Solubilization of Single-Wall Carbon Nanotubes in Water. *Nano Lett*. **2003**, 3, 269-273.

Maitra, U.; Gomathi, A.; Rao, C. N. R. Covalent and Noncovalent Functionalisation and Solubilisation of Nanodiamond. *J. Exp. Nanosci*. **2008**, 3, 271-278.

Maitra, U.; Prasad, K. E.; Ramamurty, U.; Rao, C. N. R. Mechanical Properties of Nanodiamond-Reinforced Polymer-Matrix Composites. *Solid State Commun*. **2009**, 149, 1693-1697.

Manivannan, S.; Jeong, I. O.; Ryu, J. H.; Lee, C. S.; Kim, K. S.; Jang, J.; Park, K. C. Dispersion of Single-Walled Carbon Nanotubes in Aqueous and Organic Solvents through a Polymer Wrapping Functionalization. *J. Mater. Sci.: Mater. Electron*. **2009**, 20, 223-229.

Martínez, M. T.; Tseng, Y.-C.; Ormategui, N.; Loinaz, I.; Eritja, R.; Bokor, J. Label-Free DNA Biosensors Based on Functionalized Carbon Nanotube Field Effect Transistors. *Nano Lett*. **2009**, 9, 530-536.

Mehta, S. K.; Kaur, G.; Bhasin, K. K. Analysis of Tween Based Microemulsion in the Presence of Tb Drug Rifampicin. *Colloids Surf., B*. **2007**, 60, 95-104.

Meng, X.; Chen, Y.; Chowdhury, S. R.; Yang, D.; Mitra, S. Stabilizing Dispersions of Hydrophobic Drug Molecules Using Cellulose Ethers During Anti-Solvent Synthesis of Micro-Particulates. *Colloids Surf., B.* **2009**, 70, 7-14.

Merisko-Liversidge, E.; Liversidge, G. G.; Cooper, E. R. Nanosizing: A Formulation Approach for Poorly-Water-Soluble Compounds. *Eur. J. Pharm. Sci*. **2003**, 18, 113-120.

Mersmann, A. Crystallization and Precipitation. *Chem. Eng. Process.* **1999**, 38, 345-353.

Meyers, J. D.; Doane, T.; Burda, C.; Basilion, J. P. Nanoparticles for Imaging and Treating Brain Cancer. *Nanomedicine*. **2013**, 8, 123-143.

Mine, E.; Nagao, D.; Kobayashi, Y.; Konno, M. Solvent Effects on Particle Formation in Hydrolysis of Tetraethyl Orthosilicate. *J. Sol-Gel Sci. Technol*. **2005**, 35, 197-201.

Mochalin, V. N.; Shenderova, O.; Ho, D.; Gogotsi, Y. The Properties and Applications of Nanodiamonds. *Nat. Nano*. **2012**, 7, 11-23.

Motshekga, S. C.; Pillai, S. K.; Sinha Ray, S.; Jalama, K.; Krause, R. W. M. Recent Trends in the Microwave-Assisted Synthesis of Metal Oxide Nanoparticles Supported on Carbon Nanotubes and Their Applications. *J. Nanomater*. **2012**, 691503, 1-31.

Muhrer, G.; Meier, U.; Fusaro, F.; Albano, S.; Mazzotti, M. Use of Compressed Gas Precipitation to Enhance the Dissolution Behavior of a Poorly Water-Soluble Drug: Generation of Drug Microparticles and Drug-Polymer Solid Dispersions. *Int. J. Pharm.* **2006**, 308, 69-83.

Nagata, A.; Oku, T.; Kikuchi, K.; Suzuki, A.; Yamasaki, Y.; Osawa, E. Fabrication, Nanostructures and Electronic Properties of Nanodiamond-Based Solar Cells. *Prog.Nat. Sci. Mater. Int*. **2010**, 20, 38-43.

Neitzel, I.; Mochalin, V.; Knoke, I.; Palmese, G. R.; Gogotsi, Y. Mechanical Properties of Epoxy Composites with High Contents of Nanodiamond. *Compos. Sci. Technol*. **2011**, 71, 710-716.

Nguyen, T. T.-B.; Chang, H.C.; Wu, V. W.-K. Adsorption and Hydrolytic Activity of Lysozyme on Diamond Nanocrystallites. *Diamond Relat. Mater*. **2007**, 16, 872-876.

Niyogi, S.; Boukhalfa, S.; Chikkannanavar, S. B.; McDonald, T. J.; Heben, M. J.; Doorn, S. K. Selective Aggregation of Single-Walled Carbon Nanotubes Via Salt Addition. *J. Am. Chem. Soc.* **2007**, 129, 1898-1899.

Noguchi, Y.; Fujigaya, T.; Niidome, Y.; Nakashima, N. Single-walled Carbon Nanotubes DNA Hybrids in Water are Highly Stable. *Chem. Phys. Lett.* **2008**, 455, 249-251.

O'Connell, M. J.; Boul, P.; Ericson, L. M.; Huffman, C.; Wang, Y.; Haroz, E.; Kuper, C.; Tour, J.; Ausman, K. D.; Smalley, R. E. Reversible Water-Solubilization of Single-Walled Carbon Nanotubes by Polymer Wrapping. *Chem. Phys. Lett*. **2001**, 342, 265-271.

O'Shaughnessy, P. T. Occupational Health Risk to Nanoparticulate Exposure. *Environ. Sci.: Processes Impacts*. **2013**, 15, 49-62.

Osawa, E. Monodisperse Single Nanodiamond Particulates. *Pure. Appl. Chem*. **2008**, 80, 1365-1379.

Osswald, S.; Havel, M.; Gogotsi, Y. Monitoring Oxidation of Multiwalled Carbon Nanotubes by Raman Spectroscopy. *J. Raman Spectrosc*. **2007**, 38, 728-736.

Patrick Augustijns, M. B. 2007. Solvent Systems and Their Selection in Pharmaceutics and Biopharmaceutics, Springer.

Pavlova-Verevkina, O. B.; Ozerina, L. A.; Politova, E. D.; Surin, N. M; Ozerin, A. N. Effect of Electrolytes on the Slow Aggregation of TiO_2 Nanocrystals. *Colloid J.* **2009**, 71, 529-533.

Peng, X.; Jia, J.; Gong, X.; Luan, Z.; Fan, B. Aqueous Stability of Oxidized Carbon Nanotubes and the Precipitation by Salts. *J. Hazard. Mater*. **2009**, 165, 1239-1242.

Petrov, P.; Lou, X.; Pagnoulle, C.; Jérôme, C.; Calberg, C.; Jérôme, R. Functionalization of Multi-Walled Carbon Nanotubes by Electrografting of Polyacrylonitrile. *Macromol. Rapid Commun*. **2004**, 25, 987-990.

Pongpeerapat, A.; Itoh, K.; Tozuka, Y.; Moribe, K.; Oguchi, T.; Yamamoto, K. Formation and Stability of Drug Nanoparticles Obtained from Drug/PVP/SDS Ternary Ground Mixture. *J Drug Deliv. Sci. Technol*. **2004**, 14, 441-447.

Popescu, B. M.; Ali, N.; Basturea, G.; Comsa, G. I.; Materon, L. A.; Chipara, M. 1-Dimensional Nanoparticles - a Brief Critical Review on Biological, Medical, and Toxicological Aspects. *Appl. Surf. Sci*. **2013** (In Press).

Rabinow, B. E. Nanosuspensions in Drug Delivery. *Nat. Rev. Drug Discovery.* **2004**, 3, 785-796.

Rasenack, N. Müller, B. W. Dissolution Rate Enhancement by in Situ Micronization of Poorly Water-Soluble Drugs. *Pharm. Res.* **2002**, 19, 1894-1900.

Saleh, N. B.; Pfefferle, L. D.; Elimelech, M. Aggregation Kinetics of Multiwalled Carbon Nanotubes in Aquatic Systems: Measurements and Environmental Implications. *Environ. Sci. Technol*. **2008**, 42, 7963-7969.

Sanganwar, G. P.; Sathigari, S.; Babu, R. J.; Gupta, R. B. Simultaneous Production and Co-Mixing of Microparticles of Nevirapine with Excipients by Supercritical Antisolvent Method for Dissolution Enhancement. *Eur. J. Pharm. Sci*. **2010**, 39, 164-174.

Sano, M.; Kamino, A.; Shinkai, S. Critical Coagulation of Langmuir Monolayers: 2D Schulze-Hardy Rule. *J. Phys. Chem. B*. **2000**, 104, 10339-10347.

Sano, M.; Okamura, J.; Shinkai, S. Colloidal Nature of Single-Walled Carbon Nanotubes in Electrolyte Solution: The Schulze-Hardy Rule. *Langmuir*. **2001**, 17, 7172-7173.

Schmidt, C.; Bodmeier, R. Incorporation of Polymeric Nanoparticles into Solid Dosage Forms. *J. Controlled Release*. **1999**, 57, 115-125.

Schrand, A. M.; Hens, S. A. C.; Shenderova, O. A. Nanodiamond Particles: Properties and Perspectives for Bioapplications. *Crit. Rev. Solid State Mater. Sci*. **2009**, 34, 18-74.

Shenderova, O. Ciftan Hens, S. 2010 Detonation Nanodiamond Particles Processing, Modification and Bioapplications. Springer, New York ,New York, US**A.**

Shenderova, O.; Zhirnov, V.; Brenner, D. Carbon Nanostructures. *Crit. Rev. Solid State Mater. Sci*. **2002**, 27, 227-356.

Shenderova, O.; Grichko, V.; Hens, S.; Walch, J. Detonation Nanodiamonds as UV Radiation Filter. *Diamond Relat. Mater*. **2007**, 16, 2003-2008.

Shieh, Y. T.; Liu, G. L.; Wu, H. H.; Lee, C. C. Effects of Polarity and PH on the Solubility of Acid-Treated Carbon Nanotubes in Different Media. *Carbon*. **2007**, 45, 1880-1890.

Smith, B.; Wepasnick, K.; Schrote, K. E.; Bertele, A. R.; Ball, W. P.; O'Melia, C.; Fairbrother, D. H. Colloidal Properties of Aqueous Suspensions of Acid-Treated, Multi-Walled Carbon Nanotubes. *Environ. Sci. Technol*. **2009**, 43, 819-825.

Spitsyn, B. V.; Davidson, J. L.; Gradoboev, M. N.; Galushko, T. B.; Serebryakova, N. V.; Karpukhina, T. A.; Kulakova, I. I.; Melnik, N. N. Inroad to Modification of Detonation Nanodiamond. *Diamond Relat. Mater*. **2006**, 15, 296-299.

Sultana, S.; Khan, M. R.; Kumar, M.; Kumar, S.; Ali, M. Nanoparticles-Mediated Drug Delivery Approaches for Cancer Targeting: A Review. *J. Drug. Target*. **2013**, 21, 107-125.

Sun, Y. P.; Fu, K.; Lin, Y.; Huang, W. Functionalized Carbon Nanotubes: Properties and Applications. *Acc. Chem. Res*. **2002**, 35, 1096-1104.

Thess, A.; Lee, R.; Nikolaev, P.; Dai, H.; Petit, P.; Robert, J.; Xu, C.; Lee, Y. H.; Kim, S. G.; Rinzler, A. G.; Colbert, D. T.; Scuseria, G. E.; Tománek, D.; Fischer, J. E.; Smalley, R. E. Crystalline Ropes of Metallic Carbon Nanotubes. *Science*. **1996**, 273, 483-487.

Thostenson, E. T.; Chou, T. W. Microwave Processing: Fundamentals and Applications. *Compos. Part A., Appl. Sci. Manuf*. **1999**, 30, 1055-1071.

Tóth, J.; Kardos-Fodor, A.; Halász-Péterfi, S. The Formation of Fine Particles by Salting-out Precipitation. *Chem. Eng. Process.* **2005**, 44, 193-200.

Tu, J. S.; Perevedentseva, E.; Chung, P. H.; Cheng, C. L. Size-Dependent Surface Co Stretching Frequency Investigations on Nanodiamond Particles. *J. Chem. Phys*. **2006**, 125, 174713-174720.

Turner, S.; Lebedev, O. I.; Shenderova, O.; Vlasov, I. I.; Verbeeck, J.; Van Tendeloo, G. Determination of Size, Morphology, and Nitrogen Impurity Location in Treated Detonation Nanodiamond by Transmission Electron Microscopy. *Adv. Funct. Mater.* **2009**, 19, 2116-2124.

Ushizawa, K.; Sato, Y.; Mitsumori, T.; Machinami, T.; Ueda, T.; Ando, T. Covalent Immobilization of DNA on Diamond and Its Verification by Diffuse Reflectance Infrared Spectroscopy. *Chem. Phys. Lett*. **2002**, 351, 105-108.

Valentini, L.; Puglia, D.; Armentano, I.; Kenny, J. M. Sidewall Functionalization of Single-Walled Carbon Nanotubes through Cf4 Plasma Treatment and Subsequent Reaction with Aliphatic Amines. *Chem. Phys. Lett.* **2005**, 403, 385-389.

Van Eerdenbrugh, B.; Froyen, L.; Van Humbeeck, J.; Martens, J. A.; Augustijns, P.; Van den Mooter, G. Drying of Crystalline Drug Nanosuspensions-the Importance of Surface Hydrophobicity on Dissolution Behavior Upon Redispersion. *Eur. J. Pharm. Sci*. **2008**, 35, 127-135.

Van Hoecke, K.; De Schamphelaere, K. A. C.; Ali, Z.; Zhang, F.; Elsaesser, A.; Rivera-Gil, P.; Parak, W. J.; Smagghe, G.; Howard, C. V.; Janssen, C. R. Ecotoxicity

and Uptake of Polymer Coated Gold Nanoparticles. *Nanotoxicology*. **2013**, 7, 37-47.

Van Thiel, M.; Ree, F. H. Properties of Carbon Clusters in TNT Detonation Products: Graphite-Diamond Transition. *J. Appl. Phys*. **1987**, 62, 1761-1767.

Verwey, E. J. W.; Overbeek, J. T. G. **1999**. Theory of the Stability of Lyophobic Colloids, Dover Publications.

Wang, S. G.; Zhang, Q.; Yoon, S. F.; Ahn, J.; Yang, D. J.; Wang, Q.; Zhou, Q.; Li, J. Q. Electron Field Emission from Carbon Nanotubes and Undoped Nano-Diamond. *Diamond Relat. Mater*. **2003**, 12, 8-14.

Wang, Y.; Dave, R. N.; Pfeffer, R. Polymer Coating/Encapsulation of Nanoparticles Using a Supercritical Anti-Solvent Process. *J. Supercrit. Fluids.* **2004**, 28, 85-99.

Wang, Y.; Iqbal, Z.; Mitra, S. Rapidly Functionalized, Water-Dispersed Carbon Nanotubes at High Concentration. *J. Am. Chem. Soc*. **2005a**, 128, 95-99.

Wang, Y.; Iqbal, Z.; Mitra, S. Microwave-Induced Rapid Chemical Functionalization of Single-Walled Carbon Nanotubes. *Carbon*. **2005b**, 43, 1015-1020.

Wang, Y.; Iqbal, Z.; Mitra, S. Rapid, Low Temperature Microwave Synthesis of Novel Carbon Nanotube-Silicon Carbide Composite. *Carbon*. **2006**, 44, 2804-2808.

Welz, S.; Gogotsi, Y.; McNallan, M. J. Nucleation, Growth, and Graphitization of Diamond Nanocrystals During Chlorination of Carbides. *J. Appl. Phys*. **2003**, 93, 4207-4214.

Wiesbrock, F.; Hoogenboom, R.; Schubert, U. S. Microwave-Assisted Polymer Synthesis: State-of-the-Art and Future Perspectives. *Macromol. Rapid. Commun*. **2004**, 25, 1739-1764.

Wiesner, M. R.; Lowry, G. V.; Alvarez, P.; Dionysiou, D.; Biswas, P. Assessing the Risks of Manufactured Nanomaterials. *Environ. Sci. Technol*. **2006**, 40, 4336-4345.

Williams, O. A.; Nesladek, M.; Daenen, M.; Michaelson, S.; Hoffman, A.; Osawa, E.; Haenen, K.; Jackman, R. B. Growth, Electronic Properties and Applications of Nanodiamond. *Diamond Relat. Mater*. **2008**, 17, 1080-1088.

Wong, S. M.; Kellaway, I. W.; Murdan, S. Enhancement of the Dissolution Rate and Oral Absorption of a Poorly Water Soluble Drug by Formation of Surfactant-Containing Microparticles. *Int. J. Pharm.* **2006**, 317, 61-68.

Xia, D.; Quan, P.; Piao, H.; Piao, H.; Sun, S.; Yin, Y.; Cui, F. Preparation of Stable Nitrendipine Nanosuspensions Using the Precipitation–Ultrasonication Method for Enhancement of Dissolution and Oral Bioavailability. *Eur. J. Pharm. Sci.* **2010**, 40, 325-334.

Yagi, N.; Terashima, Y.; Kenmotsu, H.; Sekikawa, H.; Takada, M. Issolution Behavior of Probucol from Solid Dispersion Systems of Probucol-Polyvinylpyrrolidone. *Chem. Pharm. Bull.* **1996**, 44, 241-244.

Yang, G. W.; Wang, J. B.; Liu, Q. X. Preparation of Nano-Crystalline Diamonds Using Pulsed Laser Induced Reactive Quenching. *J. Phys.: Condens. Matter*. **1998**, 10, 7923-7927.

Yang, Q. H.; Gale, N.; Oton, C. J.; Li, H.; Nandhakumar, I. S.; Tang, Z. Y.; Brown, T.; Loh, W. H. Deuterated Water as Super Solvent for Short Carbon Nanotubes Wrapped by DNA. *Carbon*. **2007**, 45, 2701-2703.

Yu, S.-J.; Kang, M.-W.; Chang, H.-C.; Chen, K.-M.; Yu, Y.-C. Bright Fluorescent Nanodiamonds: No Photobleaching and Low Cytotoxicity. *J. Am. Chem. Soc*. **2005**, 127, 17604-17605.

Zambaux, M. F.; Bonneaux, F.; Gref, R.; Maincent, P.; Dellacherie, E.; Alonso, M. J.; Labrude, P.; Vigneron, C. Influence of Experimental Parameters on the Characteristics of Poly(Lactic Acid) Nanoparticles Prepared by a Double Emulsion Method. *J. Controlled Release*. **1998**, 50, 31-40.

Zapol, P.; Sternberg, M.; Curtis, L. A.; Frauenheim, T.; Gruen, D. M. Tight-Binding Molecular-Dynamics Simulation of Impurities in Ultrananocrystalline Diamond Grain Boundaries. *Phys. Rev. B: Condens. Matter Mater. Phys.* **2002**, 65, 454031-4540311.

Zhang, A.; Tang, M.; Luan, J.; Li, J. Noncovalent Functionalization of Multi-Walled Carbon Nanotubes with Amphiphilic Polymers Containing Pyrene Pendants. *Mater. Lett*. **2012**, 67, 283-285.

Zhang, H. X.; Wang, J. X.; Zhang, Z. B.; Le, Y.; Shen, Z. G.; Chen, J. F. Micronization of Atorvastatin Calcium by Antisolvent Precipitation Process. *Int. J. Pharm*. **2009**, 374, 106-113.

Zhang, M.; Su, L.; Mao, L. Surfactant Functionalization of Carbon Nanotubes (CNTs) for Layer-by-Layer Assembling of Cnt Multi-Layer Films and Fabrication of Gold Nanoparticle/CNT Nanohybrid. *Carbon*. **2006**, 44, 276-283.

Zhu, W.; Romanski, F. S.; Meng, X.; Mitra, S.; Tomassone, M. S. Atomistic Simulation Study of Surfactant and Polymer Interactions on the Surface of a Fenofibrate Crystal. *Eur. J. Pharm. Sci*. **2011**, 42, 452-461.

Zhu, Y.; Xu, F.; Shen, J.; Wang, B.; Xu, X.; Shao, J. Study on the Modification of Nanodiamond with DN-10. *J. Mater. Sci. Technol*. **2007**, 23, 599-603.

Zimmermann, A.; Elema, M. R.; Hansen, T.; Müllertz, A.; Hovgaard, L. Determination of Surface-Adsorbed Excipients of Various Types on Drug Particles Prepared by Antisolvent Precipitation Using HPLC with Evaporative Light Scattering Detection. *J. Pharm. Biomed. Anal*. **2007**, 44, 874-880.